

Review

Current Methods for Synthesis and Potential Applications of Cobalt Nanoparticles: A Review

Andrey A. Vodyashkin ^{1,*}, Parfait Kezimana ^{1,2}, Fedor Y. Prokonov ¹, Ivan A. Vasilenko ¹
and Yaroslav M. Stanishevskiy ¹

¹ Institute of Biochemical Technology and Nanotechnology, Peoples Friendship University of Russia (RUDN University), 117198 Moscow, Russia; kezimana-p@rudn.ru (P.K.); 1032206643@rudn.ru (F.Y.P.); vasilenko-ia@rudn.ru (I.A.V.); stanishevskiy_yam@pfur.ru (Y.M.S.)

² Department of Agrobiotechnology, Peoples Friendship University of Russia (RUDN University), Miklukho-Maklaya str. 6, 117198 Moscow, Russia

* Correspondence: vodyashkin_aa@pfur.ru

Abstract: Cobalt nanoparticles (CoNPs) are promising nanomaterials with exceptional catalytic magnetic, electronic, and chemical properties. The nano size and developed surface open a wide range of applications of cobalt nanoparticles in biomedicine along with those properties. The present review assessed the current environmentally friendly synthesis methods used to synthesize CoNPs with various properties, such as size, zeta potential, surface area, and magnetic properties. We systematized several methods and provided some examples to illustrate the synthetic process of CoNPs, along with the properties, the chemical formula of obtained CoNPs, and their method of analysis. In addition, we also looked at the potential application of CoNPs from water purification cytostatic agents against cancer to theranostic and diagnostic agents. Moreover, CoNPs also can be used as contrast agents in magnetic resonance imaging and photoacoustic methods. This review features a comprehensive understanding of the synthesis methods and applications of CoNPs, which will help guide future studies on CoNPs.

Keywords: cobalt nanoparticles; synthesis of cobalt nanoparticles; applications of cobalt nanoparticles; contrast agent; cytostatic; diagnostic and theranostic agent

Citation: Vodyashkin, A.A.; Kezimana, P.; Prokonov, F.Y.; Vasilenko, I.A.; Stanishevskiy, Y.M. Current Methods for Synthesis and Potential Applications of Cobalt Nanoparticles: A Review. *Crystals* 2022, 12, 272. <https://doi.org/10.3390/cryst12020272>

Academic Editor: Abdullah Mohamed Asiri

Received: 5 January 2022

Accepted: 14 February 2022

Published: 17 February 2022

Publisher's Note: MDPI stays neutral with regard to jurisdictional claims in published maps and institutional affiliations.



Copyright: © 2022 by the authors. Licensee MDPI, Basel, Switzerland. This article is an open access article distributed under the terms and conditions of the Creative Commons Attribution (CC BY) license (<https://creativecommons.org/licenses/by/4.0/>).

1. Introduction

In recent years, there has been a tendency towards developing and applying new materials with new properties [1,2], with particular attention paid to nanomaterials and nanoparticles [3–5] due to their several unique properties, which make them applicable in various fields—from microelectronics to biomedicine [6–8].

Currently, several methods are used to prepare various nanoparticles, including metals, non-metals, and polymeric substances [9–11], with particular attention paid to metal nanoparticles, which can be used directly or as part of hybrid material [12,13] with the developed surface, optical, magnetic, electronic, and catalytic properties.

Various physical and chemical processes are commonly used to produce and modify metallic nanoparticles. The correct selection of the method for obtaining nanoparticles strongly affects the crystal structure, surface area, size, and other properties [14]. In addition, thanks to post-synthetic modification, nanoparticles can be modified for specific tasks (for example, PEG coating to improve biocompatibility) [15].

Cobalt is a vital element but is present in small quantities in the body of a mammal and usually is provided in a diet of green vegetables and grains [16]. Key among its biological activity is its role in vitamin B12, cobalamin, as well as in a small amount of other cobalt-containing enzymes identified to date [17]. Due to the importance of cobalt in the human metabolic process, various materials based on cobalt suitable for biomedical purposes are becoming more and more relevant [18].

Cobalt nanoparticles can be used for energy storage, as catalysts, in medicine, in microelectronics, as contrast agents, and as a basis for drug delivery systems [19–22]. An essential factor is that cobalt nanoparticles can be magnetic [23], which opens up new possibilities for using nanoparticles as a carrier for targeted drug delivery [24]. It should also be noted that due to their physico-chemical properties and small size, cobalt nanoparticles can be successfully used as sensors to determine various substances [25].

Due to the simplicity of obtaining cobalt nanoparticles and their high applied value in many industries, in this review, we looked at the main synthesis methods of cobalt/cobalt oxide nanoparticles and their application from catalysis to the main biomedical applications of cobalt nanoparticles, such as anticancer therapy and diagnostic materials.

2. Synthesis Methods of CoNPs

Currently, there is great interest in developing new methods for producing cobalt nanoparticles due to the high applied significance of nanoparticles in various spheres of human life [26,27]. Modern methods of obtaining nanoparticles of cobalt must meet several key indicators that ensure high efficiency of the developed process:

1. High yield of the target product,
2. The possibility of obtaining nanoparticles of a given structure (crystallinity, size, shape)
3. Safety and practicality of the method of obtaining
4. Environmentally friendly methods
5. Scalability

All methods of cobalt nanoparticles preparation can be divided into four categories: physical, chemical, physicochemical, and biological (Figure 1). Different approaches should be applied to meet the specific challenges faced during the synthesis.

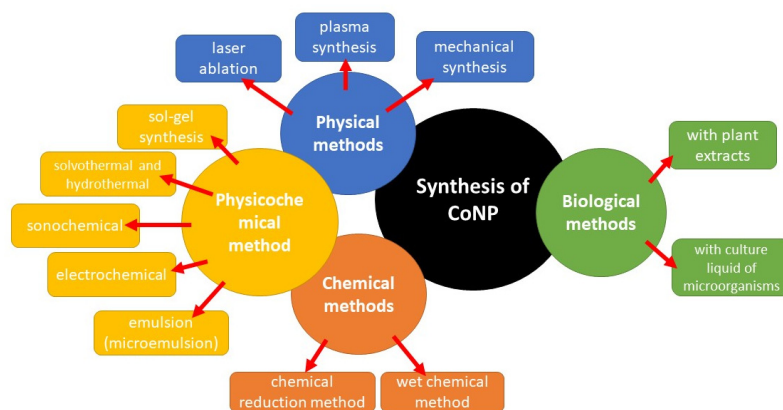


Figure 1. Main methods for the synthesis of cobalt nanoparticles.

2.1. Solution Method of CoNPs Synthesis

The solution method is a method for producing cobalt nanoparticles. The formation of nanoparticles occurs directly in the liquid phase (solution) under the influence of various factors, temperature, pressure, mixing modes, etc.

Particular attention is paid to the choice of the capping agent. The stabilizing agent is adsorbed on the surface of nanoparticles due to non-covalent bonds. Capping agent plays an important role in stabilizing nanoparticles and preventing their aggregation. Table 1 lists the main stabilizing agents used to prepare various cobalt nanoparticles.

Table 1. Capping agents and synthesis' methods of CoNPs.

No.	Capping Agent	Size	Chemical Formula	Method of Analysis	Shape	References
Wet Chemical Method						
1	Tetrabutyl ammonium bromide	80–100 nm	Co(0)	XRD	Spherical	[28]
2	Without use capping agent	10–20 nm	Co(0)	XRD	Spherical	[29]
3	Without use capping agent	20–40 nm	CoO	XPS	Spherical	[30]
4	Without use capping agent	20 nm	Co(0)	XRD	Hexagonal and quadrilateral	[31]
5	Oleic acid	3–4 nm	Co(0)	-	Spherical, uniform shape	[32]
Hydrothermal Method						
6	Oleic acid	1–10 nm	Co(0), CoO < 5%	XRD	Spherical	[33]
7	Without use capping agent	20–400 nm	CoO	XRD	Spherical	[34]
8	Without use capping agent	3–4 nm	CoO, Co ₃ O ₄	XRD	Hexagonal nanocrystals	[35]
9	Sodium dodecyl sulfate	20 nm	Co ₃ O ₄	XRD	Cubic shape	[36]
10	Trioctylphosphane, oleic acid	150–300 nm	Co(0)	XRD	Nanowire	[37]
Solvothermal Method						
11	Without use capping agent	2 nm	Co(0)	XRD	Spherical	[38]
12	Oleylamine	100–120 nm	Co(0)	XRD	Spherical, hexagonal nanocrystals	[39]
13	Without use capping agent	10–30 nm	CoO, Co ₃ O ₄	XRD	Cubic-shape, spherical	[40]
14	Oleylamine, oleic acid	5–30 nm	Co(0)	WAXS, HREM	Nanorods, nanowires	[41]
15	Without use capping agent	50–75 nm	Co(0)	XRD	Spherical	[42]
16	Without use capping agent	1.5 nm	Co(0)	HREM	Spherical	[43]
17	Without use capping agent	79 ± 17 nm 11 ± 3 nm	Co(0)	XRD	Cubic shape spherical	[44]
Sol-gel method						
18	Citric acid and oleic acid	8–12 nm	Co ₃ O ₄	XRD	Cubic crystal	[45]
19	Oleylamine	20 ± 3	CoO	XRD	Hollow nanoparallelepiped	[46]
Electroless Deposition (Chemical Reduction) in Solution						
20	3- (N, N-dimethyldodecylammonia) propanesulfonate	3–5 nm	Co(0)	XRD	Hexagonal	[47]
21	Sodium citrate dihydrate	400 nm	Co(0)	XRD	Hexagonal	[48]
22	Without use capping agent	100–120 nm	Co, CoO, Co ₃ O ₄	XRD	Spherical	[49]
23	3- (N, N-dimethyldodecylammonia) propanesulfonate	3–5 nm	Co(0)	XRD	Hexagonal	[50]
24	Without use capping agent	2.2–4.2 nm	Co(0)	XPS	Spherical	[51]

25	Chloroplatinic acid hexahydrate	24–110 nm	CoO	XRD	Hexagonal	[52]
Electrochemical Method						
26	Sodium formate	2 nm	CoO	XRD	Spherical	[53]
Electrosynthesis of Metal in a Liquid Phase Reduction of Their Ions or Complexes						
27	Tetrabutylammonium chloride	5–100 nm	CoO, Co ₃ O ₄	EDX, XRD	Spherical	[54]
Galvanic Replacement Method						
28	Sodium citrate dihydrate	100–120 nm	Co(0)	EDX	Spherical, hollow nanoparticles	[55]
Liquid Phase Plasma Reduction Method						
29	Chloroplatinic acid hexahydrate	24–112 nm	Co(0), CoO, Co ₃ O ₄	EDX, XRD	Spherical	[56]
30	Without use capping agent	10 nm	CoO	XRD	Spherical	[57]

The most commonly used stabilizing agent for cobalt nanoparticles is oleic acid, which has been used in most works since the early 2000s [58,59].

Barbara Farkas et al. [23] studied the mechanism of interaction of carboxylic acids with a cluster of cobalt nanoparticles using ab initio modeling. Their study used valeric acid to analyze the reaction of a carboxylic acid with NPs. They found that a carboxylic acid interacting with the surface of CoNPs forms a monodentant bond due to oxygen, which loses its bond with hydrogen during dissociation. Furthermore, during the simulation, the formation of bridging bidentate interactions was observed using chelation between the second oxygen atom and cobalt, which prevents cluster aggregation [23].

Cobalt nanoparticles were obtained by chemical reduction using sodium borohydride [28]. First, cobalt sulfate, tetrabutylammonium bromide, and deionized water were added to a glass flask at room temperature with stirring. Next, a 0.1 M sodium borohydride solution was added to the solution. The mixture was stirred for 15 min, then the aqueous solution was decanted, and the resulting particle was washed with water and acetone, thus preparing spherical nanoparticles of 80–100 nm in size. The obtained particles were spherical; the EDX (Energy Dispersive X-Ray spectroscopy) showed the presence of cobalt and oxygen, which indicates that the obtained nanosized cobalt has the formula Co(0), an oxidized layer on the surface of the nanoparticles.

This method is the simplest for the preparation of nanoparticles since it does not require sophisticated equipment and does not require special conditions for carrying out the reactions and preparing nanoparticles, widely used in various fields [60].

Another method for obtaining cobalt nanoparticles is the thermal decomposition of organic cobalt salts in the presence of a capping agent [31,61]. The decomposition of octacarbonyl dicobalt has synthesized cobalt nanoparticles. In a vacuum, trioctylphosphine oxide was heated to 80 °C, to which 1,2-dichlorobenzene and oleic acid were added; and the mixture was heated to 180 °C under a nitrogen atmosphere. Next, dicobalt octacarbonyl, previously dissolved in 1,2-dichlorobenzene, was introduced into the mix with vigorous stirring and kept at 180 °C for another 15 min, and the nanoparticles were precipitated with ethanol. Cobalt nanoparticles were isolated by centrifugation, and as a result, spherical cobalt nanoparticles with a size of 7–8 nm were obtained [31]. Still, there were no data on the crystallographic structure of the NPs. The method allows one to get nanoparticles with a narrow size distribution. However, it is challenging to implement. It is also worth noting that the use of octacarbonyl in this synthesis of dicobalt is dangerous due to its high toxicity [61,62]. To avoid using toxic compounds, Masoud Salavati-Niasari et al. [61] prepared cobalt nanoparticles by thermal decomposition of cobalt coordination compounds. The bis (salicylaldiminato) cobalt (II)-oleylamine complex was preliminarily obtained by mixing 0.6 g of bis (salicylaldiminato) cobalt (II) and 2 mL of oleylamine with

stirring, and then placed in a three-necked distillation flask and heated to 100 °C for 90 min. The flask was purged with high purity argon gas to avoid oxidation throughout the entire process. To obtain cobalt nanoparticles, triphenylphosphine was added to the resulting solution of the metal complex at 220 °C. The solution was kept at 210 °C for 45 min and then cooled to room temperature. Nanoparticles were precipitated by adding excess ethanol to the solution, and as a result spherical cobalt nanoparticles with sizes ranging from 25 to 35 nm were obtained [61]. XRD (X-ray diffraction analysis) data from freshly prepared nanoparticles showed no cobalt oxides. However, after exposure of the nanoparticles to air, the presence of cubic cobalt oxides CoO and Co₃O₄ was seen in the X-ray diffraction pattern, while Co(0) was completely absent. Although, this method produces nanoparticles with a wide distribution, it has advantages too, as it allows you to control the size of the resulting particles by changing the ratio of the precursor and stabilizing agent.

2.1.1. Hydrothermal Method of CoNPs Synthesis

The hydrothermal method was used by S. M. Ansari et al. to prepare cobalt nanoparticles [33]. First, cobalt chloride was dissolved in deionized water, and a KOH solution was added, followed by stirring for at least 15 min. Then solutions of hydrazine monohydrate and oleic acid were added so that the total volume of the mixture was 2/3 of the total volume of the autoclave, the resulting mixture was kept under stirring for 2 h until the solid reagents were dissolved entirely, and then the mixture was poured into a Teflon-coated autoclave and placed into an electric oven, where the reaction temperature was maintained at 160 °C for 24 h. After 24 h, the autoclave was allowed to cool naturally to room temperature. Finally, the obtained CoNPs were separated from the liquid phase by centrifuging the final solution, decanting the liquid phase, and drying the resulting black precipitate in an oven at 100 °C [33]. The average size of the obtained NPs was 192 nm, and the XRD data showed that the crystal structure of the NPs is hexagonal and cubic, and the presence of only Co(0) was also revealed.

The present method is more convenient in application and easily scalable. Moreover, it allows one to obtain spherical nanoparticles with a narrow size distribution, which can be helpful in various areas of medicine.

G. Seong et al. [34] prepared CoNPs with a supercritical hydrothermal reduction and the decomposition of formic acid (at temperature up to 420 °C, and a pressure of 22 MPa), and to avoid contact with air, the introduction of precursors into the autoclave was carried out in an insulator in an argon atmosphere. An aqueous solution of cobalt acetate and formic acid was loaded into an autoclave, placed in an electronic oven, and heated to 430 °C for 10 min. After 10 min, the autoclave was cooled in a water bath at the temperature of 25 °C for 5 min to prevent particle growth. The cooled autoclave was opened to allow the resulting gases to escape and closed again. Nanoparticles were precipitated by adding methanol, centrifuged, and washed with methanol. The resulting particles ranged from 20 to 400 nm and had a spherical shape. A thermodynamic analysis of the system was performed and proved that the experimental data agree with the data calculated using the PSRK EOS [34]. According to XRD data, the structure contains metallic cobalt and weak peaks of cobalt oxide CoO. Water in a supercritical state is a universal environmentally friendly solvent that is non-toxic and nonflammable. The synthesis conditions can be controlled since water's density and dielectric constant change significantly near its critical point. This synthesis is environmentally friendly, but it should be noted that this method requires special equipment and increased safety measures due to the use of supercritical conditions.

2.1.2. The Solvothermal Method of CoNPs Synthesis

The solvothermal method is similar in its technology to the hydrothermal one, as it is also carried out in autoclaves at high temperature and pressure, with just one difference, instead of water, the synthesis is carried out in organic solvents. The method was used by

M. Alagiri et al. [38] to synthesize CoNPs. First, cobalt chloride was dissolved in ethanol with vigorous stirring for 2 h to obtain a homogeneous transparent purple solution. Then, a solution of hydrazine monohydrate was dropped to the resulting mixture with continuous stirring at a temperature of 50 °C. Then, triethanolamine was added to the above mixture with vigorous stirring, followed by further stirring for 2 h. Next, the mixed solution was placed in a Teflon-lined stainless-steel autoclave, sealed, and kept at 120 °C for 8 h. Then, the autoclave was allowed to cool from 120 °C to room temperature. Next, the sample was washed several times with distilled water, ethanol, and acetone. Finally, the product was dried under vacuum at 60 °C for 4 h. The resulting particles had a spherical shape, were 2 nm in size, and had the structure of metallic cobalt Co(0), while other phases were absent (according to XRD data). This method makes it possible to obtain particles of a given size without an oxide layer on the surface.

2.1.3. Microemulsion Method of CoNPs Synthesis

To improve the properties of nanoparticles, such as size, shape, particle-size distribution, and chemical composition, the microemulsion method for the synthesis of nanoparticles was developed. This method includes the preparation of nanoparticles in various heterogeneous systems with water-in-oil and oil-in-water emulsions. Several reviews on using the microemulsion method in the synthesis of nanoparticles have been prepared [63,64]. The microemulsion methods are attracting more and more attention due to the possibility of adjusting a more significant number of parameters. Still, a systematic study is needed to establish all the factors affecting the basic properties of nanoparticles. Therefore, several nanoparticles were prepared, for example, Zn [65], Sn [66], Cu [67], Ti [68], Fe [69], Ag [70], Au [71].

CoNPs and cobalt-metal alloys can be obtained using the microemulsion method, and it can be done following a typical scheme that includes active mixing of a precursor containing Co ions, such as $\text{Co}(\text{NO}_3)_2$; a surfactant, for example, CTAB (cetyltrimethylammonium bromide); an oil phase, which may include a hydrocarbon (for example, isooctane), or alcohol (for example, butanol); and an aqueous phase which may contain alkali or some other reducing agent; after which the nanoparticles are separated from the liquid phase. Another scheme of preparing cobalt nanoparticles using the microemulsion method is mixing cobalt acetate tetrahydrate dissolved in ethylene glycol. First, hydrazine hydrate and ethylene glycol are separately mixed in a separate beaker, then the prepared cobalt solution above was added dropwise to the hydrazine solution at a rate of 2 mL/min with constant stirring. The result is the formation of a pink-colored emulsion. Furthermore, to increase stability, various high-molecular substances can be added to these systems, for example, starch, polyvinylpyrrolidone (PVP), polyvinyl alcohol. To accelerate the reaction, this system can be heated. Due to the use of ethylene glycol as a solvent, the reaction can be carried out at a temperature up to 160 °C, which will allow the reaction to proceed much faster than in water systems. Furthermore, this method makes it possible to obtain nanoparticles Co(0) (according to XRD and SAXS) with an average size of 35 nm and the manifestation of magnetic properties, which makes it possible to use CoNPs in magnetic carriers [72].

As an example, Khan J. et al. [73] developed a method for obtaining CoF_2 nanoparticles. During the synthesis, water-in-oil microemulsions were prepared in two Teflon beakers by stirring 5.0 g CTAB, 30.0 g 2-octanol, and 4.0 g H_2O for one h using a magnetic stirrer. During the synthesis, two solutions were created, the first of which contained 0.58 g (2.0 mmol) of cobalt nitrate hexahydrate $[\text{Co}(\text{NO}_3)_2 \cdot 6\text{H}_2\text{O}]$, and the second contained 0.18 g (5.0 mmol) NH_4F . After stirring individually for one h, the two microemulsions were mixed, and the mixture was stirred for 1 h. Light pink precipitates were obtained after centrifuging the supernatant at 4000 rpm for 30 min. As a result, the light pink powder was washed with ethanol, then dried at room temperature for 24 h. Such NPs have high thermal stability and a homogeneous composition showing electrochemical characteristics compared to other NPs, which suggests that CoNPs can potentially be used as

cathode materials in energy storage devices and lithium-ion batteries. The other method of obtaining cobalt nanoparticles cobalt Co(0) (according to XRD data) with magnetic properties by the microemulsion method is mixing a solution of sodium bis (2-Ethylhexyl) sulfosuccinate (AOT) in gasoline and a 0.1 M aqueous solution of CoCl₂ in deionized water. The mixture was shaken until an emulsion was formed, reducing a metal ion with the formation of the corresponding metal nanoparticles. Then, a solution of 5 mL of NaBH₄ was added to the solution of metal ions. The mixture was stirred for 2 h at room temperature at 750 rpm, and then all synthesized nanoparticles were washed with excess acetone, centrifuged, and placed in an oven at 80 °C for 12 h [74].

2.2. Green Methods of CoNPs Synthesis

Recently, there has been a tendency in the scientific community to develop various green methods for materials synthesis, particularly nanoparticles. These methods increase the safety and environmental friendliness of the synthetic process. In addition, due to the unique chemical composition of biological systems, nanoparticles obtained by these methods can have unique structure and physico-chemical properties [75,76]. Another property of such nanoparticles is increased biocompatibility due to the affinity of the capping agent and substances in living organisms (microorganisms and humans), which allows the finding of new fields of application of nanoparticles in various systems [77]. One of the synthesis methods of nanoparticles using green chemistry is reducing cobalt precursors using extracts of different plants. The plant extracts can be both aqueous and organic solvents and act as a reducing agent and a capping agent for the resulting cobalt nanoparticles. Due to a set of extractable compounds, this method provides unique structures and high biocompatibility of the resulting nanomaterials compared to nanoparticles obtained by a synthetic method [78].

Melvin S. Samuel et al. [79] proposed a green method for producing cobalt nanoparticles using extracts from *Vitis rotundifolia*, the essence of which consisted of the gradual addition of the pulp extract to a solution of cobalt chloride, with heating and stirring. After alkalization of the resulting system, a precipitate was isolated, then dried and calcined for further use. The resulting nanoparticles had a wide size distribution. In addition, they had a polycrystalline cubic structure of Co(0) NPs, established by XRD, which may be associated with a wide range of chemicals in the extract.

Apart from plant extracts, red algae extracts have also been used to prepare cobalt nanoparticles, such as proposed by Jamaan S. Ajarem et al. [80] consists in adding cobalt nitrate dropwise to the algae extract (obtained by heating dried algae at 70 °C for 4 h in an aqueous medium), then stirring continuously at room temperature for 24 h, while the color of the solution changes from pale pink to dark brown. Ismat Bibi et al. [81] suggested a similar method for nanoparticles preparation using plant extracts. The technique consisted of mixing while heating to 70 °C the extract of the peel of *P. granatum* and the precursor of cobalt for 90 min. Then it was left overnight, after which the precipitate was separated and dried. As a result, nanoparticles with an average size of 80 nm and face-centered cubic crystalline phase of cobalt oxide (XRD data) were obtained, which showed high efficiency in the decomposition of organic dyes

In addition to these methods, there are also microbiological methods, including several methods for nanoparticle preparation using various bacteria cultures. The synthesis of CoNPs is carried out with the help of microorganisms, which capture metal ions from the solution, and then release the reduced metal with the help of enzymes. Synthesis using microbiological systems makes it possible to obtain nanoparticles on a large scale with high colloidal and sedimentation stability. For example, the method proposed by Eunjin Jang et al. [82] allows obtaining rod-shaped CoNPs on the surface of bacteria. This method consists in incubating cobalt chloride with a suspension of *Bacillus subtilis*, followed by separation and purification of cobalt nanoparticles using centrifugation and washing. This method makes it possible to obtain nanoparticles by a simple method at room temperature, and they have shown high application value for the creation of nanobiocatalysts.

Apart from bacterial cultures, fungi have also been used to prepare CoNPs, as seen in the study of Vijayanandan A. S. and Balakrishnan R. M. [83], in which nanoparticles were obtained using the fungi *Aspergillus nidulans*. The essence of this method was to maintain cobalt acetylacetonate and the fungi mycelium on a rotary shaker at room temperature for 5 days, after which the solution was filtered and washed with distilled water to remove the components of the medium. Then the nanoparticles were separated from the components of the medium by centrifugation. These nanoparticles had an average size of 20 nm and were stabilized by sulfur-containing proteins (FTIR data) isolated by *Aspergillus nidulans* during cultivation. Cobalt oxide nanoparticles were in the spinel phase according to the data from the International Center for Diffraction Data.

Another example is the work of B. A. Omran et al. [84], who used the cell-free filtrate of *Aspergillus brasiliensis* ATCC 16404 for the mycosynthesis of Co_3O_4 -NPs. The method included the cultivation of 4 mmol $\text{CoSO}_4 \cdot 7\text{H}_2\text{O}$ and 5% filtrate of *A. brasiliensis* mycelium for 72 h at pH 11 on a shaker in the dark. During the synthesis, the color of the solution changed from yellow to brown. The mycosynthesized CoNPs had a spherical shape and a size of 20–26 nm. They had antibacterial activity against several microorganisms and exhibited magnetic properties.

2.3. Physical Methods of CoNPs Synthesis

Physical methods can be used to prepare CoNPs, and they are based on the use of mechanical, optical, electronic treatments on the material to obtain various nanoobjects [85]. Physical methods for producing nanoparticles include mechanical crushing or grinding of bulk metal, vapor condensation, spray pyrolysis, flame spray pyrolysis, aerosol process, and unconventional mechanical process [86].

2.3.1. Vapor Condensation Method

A long-known method for obtaining metal nanoparticles is the vapor condensation method, which consists of organic metal salts being converted into a gaseous state under a vacuum and then condensed. The metal after such a procedure is precipitated in a reduced form [87–89]. X. L. Dong et al. obtained cobalt nanoparticles by the chemical condensation method. In the apparatus chamber for chemical vapor condensation, octacarbonyl dicobalt was evaporated at 60 °C, then a carrier gas, argon, or helium, was fed into the chamber, which transported the vapors to a tube cooled with liquid nitrogen, on which the vapors were condensed. After this procedure, the particles were scraped off the walls. As a result, both cobalt nanoparticles and cobalt oxide nanoparticles of the shape of a string and a spherical shape with a size of 10–25 nm were found in the resulting powder. In addition, the XRD results revealed the presence of metallic cobalt Co (0) [87]. In their experiment, Z. H. Wang et al. prepared cobalt nanocapsules coated with a carbon film [88], to synthesize dicobalt octacarbonyl and high-purity carbon monoxide as a carrier gas were used as a precursor. The evaporation temperature of dicobalt octacarbonyl was 60 °C. The carrier gas stream transports the precursor vapors and passes through an oven heated to temperatures between 400 and 1000 °C, in which the precursor vapors and carbon monoxide decompose and transform into nanoparticles, and then enter the cooling zone (chiller). The powders were scraped from the chiller at the end of the process. The size of the obtained nanocapsules was 20–60 nm, and the thickness of the amorphous carbon shell was 4–6 nm. XRD revealed the presence of cobalt carbide phases Co_2C , Co_3C [88]. The vapor condensation method can produce particles with a wide size distribution, but by varying the pressure in the chamber and/or the decomposition temperature during nanoparticle formation, the particle size range can be controlled.

2.3.2. The Arc Plasma-Assisted Deposition Method

The method of arc plasma-assisted deposition consists of a pulsed direct current of high power passing through a thin metal wire, which leads to an explosion of the wire. A large amount of heat energy causes the wire to melt, followed by evaporation and plasma formation. The plasma generated during the process expands and cools when it interacts with a refrigerant such as an inert gas or liquid. Then nanoparticles are formed during the nucleation process. For example, H. Meng et al. obtained cobalt nanoparticles by arc plasma evaporation. During their experiment, a metal block of cobalt was placed in a water-cooled evaporating crucible in a preparation chamber, which was pre-evacuated to 0.005 Pa and filled with a mixture of hydrogen and argon. Then a galvanic arc was ignited, and the metal melted, followed by the formation of plasma—the metal ions in the plasma collided with argon gas and condensed to form nanoparticles.

Then, the formed particles were transferred by the air flow to the separation chamber. They were separated by size; large and heavier particles settled on the surface of the chamber earlier than lighter particles. Finally, the particles were cooled to room temperature and collected in a special vacuum package for storage. The size of the obtained NPs ranged from 28 to 70 nm, and according to the XRD analysis, they consist of Co(0), with no other phases detected [90].

2.3.3. Liquid-Phase Plasma Method

The liquid-phase plasma method makes it possible to synthesize nanoparticles through an arc discharge on a metal salt solution, which forms a plasma. After the termination of the arc discharge, the plasma cools down, and as a result of nucleation, nanoparticles are formed. Hwan-Gi Kim et al. obtained cobalt nanoparticles using liquid-phase plasma [56]. Sodium laurel sulfate was used to stabilize the nanoparticles, and the liquid-phase plasma was created using an electric discharge at room temperature. A needle-shaped electrode generated a pulsed electric discharge. The duration of the plasma treatment influenced the size and the number of particles obtained. Plasma treatment of the solution for 10–60 min gave spherical nanoparticles with 10–100 nm diameter. When the solution was treated with plasma for 30 min, the diameter of the resulting spherical nanoparticles increased to 50–100 nm. When the plasma treatment lasted 60 min or more, needle-shaped crystals were formed. XRD revealed the presence of metallic cobalt Co(0) and cobalt oxides on the surface of nanoparticles [56].

Ruslan Sergiienko et al. also prepared CoNPs encapsulated in graphite using an electric plasma discharge generated in an ultrasonic cavitation field of liquid ethanol, followed by separation, drying, and annealing of the particles [57]. In the study, a cobalt plate and cobalt electrode tips were soldered to Iron electrodes and the ultrasonic homogenizer for sonication of ethanol in a glass vessel. The glass vessel was cooled in an ice bath and sealed with a Teflon lid. A stream of argon gas was fed into the vessel to maintain an inert atmosphere. During sonication, the voltage across the electrodes was held at 55 V, and the upper current limit of the source was set at 3A. Electric plasma was generated directly under the plate. In this case, the ends of the cobalt electrodes and the surface of the cobalt plate were worn out due to thermal evaporation. Then, small nanoparticles were separated from large ones dispersed in liquid ethanol using gravity settling. After the experiment, the carbonaceous powder dispersed in liquid ethanol was left to stand in a glass bottle. After a few days, nanoparticles larger than 200 nm settled on the bottom of the bottle, while smaller nanoparticles remained in the liquid ethanol dispersion. A black suspension of smaller nanoparticles poured into another bottle while the larger particles remained at the bottom of the first bottle. Smaller nanoparticles were separated from ethanol by centrifugation, and the resulting washed, and dried powder was then etched in a 15% hydrochloric acid solution for 24 h at 30 °C. The resulting nanoparticles were spherical, less than 10 nm in size, and their XRD revealed the presence of cobalt oxide CoO and cobalt carbide Co₃C phases. The use of ultrasonic irradiation in this method helped reduce

the voltage and power for generating the arc discharge and significantly reduce the particle size. Using the liquid-phase plasma method, it is possible to regulate the size and shape of the resulting nanoparticles by controlling the time of passage of the arc discharge through the solution. The complexity of this method is the need for significant energy consumption to generate a discharge, which can negatively affect the scaling of the process [57].

2.3.4. The Ultrasonic Method

The synthesis of nanomaterials using the ultrasonic method is a promising method for preparing nanomaterials, given its advantages. First, it allows intensifying the process because of acoustic cavitation when ultrasound propagates through a solution. Cavitation is a phenomenon of sequential intensive formation (increase and decrease) of vapor bubbles in a liquid. The collapse of these cavities creates local high temperatures and pressures quickly, forming hot spots in cold liquids. Cavitation is caused by high-frequency sound waves (10–120 MHz) passing through a liquid mass [91].

The use of ultrasound during nanomaterial synthesis will provide advantages based on various cavitation effects such as acoustic flow and turbulence, which enhance the Ostwald ripening process [4,92]. However, the chemical processes caused by the ultrasonic field only occur when the intensity of the ultrasound meets the conditions for the development of cavities. Despite this, the duration of ultrasonic irradiation intensities that do not reach a certain threshold does not lead to chemical reactions. Parameters include the time of exposure, pressure, temperature, ultrasound intensity, the presence of a capping agent, and the properties of the liquid phase have different effects on the formation and properties of nanomaterials. Preparation of nanomaterials using ultrasound offers several advantages that are very difficult to achieve using traditional methods such as high stability, unique morphology, crystalline nature. However, it should be noted that, at present, methods for producing nanoparticles based on ultrasonic techniques are used to a lesser extent than solution, gas-phase, thermal and emulsion methods [93].

Cobalt sulfides' sonochemical preparation: cobalt acetate dihydrate was dissolved and thioacetamide C_2H_5NS in water, then sonicated for 1 h till the red solution changed color to black. After 1 h of sonication, the black precipitate was centrifuged at 7000 rpm, washed twice with water and twice with absolute ethanol, and dried in air for 24 h. The ultrasonic methods for nanoparticles preparation can be used in conjunction with other physical treatments, such as plasma treatment, electrochemical effects, and increased pressure. M. Dabala et al. [94] proposed a method for producing cobalt-iron nanoparticles using a sonoelectrochemical process. The system consisted of a two-electrode setup, namely a titanium alloy acting as a cathode and an ultrasonic emitter connected to the potentiostat, an audio signal generator, and a platinum grid acting as an anode connected to the potentiostat. A constant galvanostatic current was applied to the sonoelectrode, and ultrasound was used with a power of up to 76 W. To produce nanopowders, the following sequence was used: A short current pulse of 0.3 and 0.5 s was applied to the sonoelectrode, and the titanium cathode acts only as an electrode. Immediately after turning off the electrochemical pulse, an ultrasonic pulse was sent to the sonoelectrode; in this case, it served only as a vibrating ultrasonic piezoelectric element; after that, there was a stage relaxation to restore the initial conditions of the process. Using this method, cobalt-iron nanoparticles were created with a cobalt content of about 65% and had a wide size distribution from 5 to 300 nm [94].

2.4. Preparation of Hybrid Materials Based on CoNPs

Hybrid materials, consisting of two or more separate components of a different nature, which after interacting, have new properties that differ from the properties of individual components. Microemulsion techniques can be used to prepare cobalt-based hybrid materials. The microemulsion system used to prepare the hybrid materials consisted of two emulsion systems differing in a metal precursor, each of which consisted of Triton

X-100 as a surfactant, propanol as an auxiliary surfactant, cyclohexane as an oil phase, an aqueous solution of hydrazine in the form of a dispersed aqueous phase and aqueous solutions of H_2PtCl_6 and CoCl_2 separately, which were then mixed and formed a cloudy microemulsion. The emulsion was then diluted to a transparent system with propanol. Nanoparticles were formed upon contact between drops containing H_2PtCl_6 and CoCl_2 and drops of a reducing solution when mixed in the presence of an oil phase. The clear solution turned black/gray due to the formation of metal nanoparticles. Pt(0)-Co(0) nanoparticles have an average size of 3–4 nm with a narrow size distribution. These nanoparticles showed high catalytic properties (better concerning methanol oxidation than pure Pt nanoparticles), which suggests the high applicability of such systems in the field of organic chemistry [95].

Another hybrid material is cobalt and carbon foam, which was prepared by a solvothermal method using cobalt acetate, which was dissolved in 80 mL of absolute ethyl alcohol. First, the crushed porous carbon foam was added to the solution and stirred for 24 h to allow the cobalt acetate to enter the foam. Next, NaOH was dissolved in ethyl alcohol, and then the solution was slowly added to the suspension and stirred for 3 h until a homogeneous suspension was formed. Next, the resulting suspension was transferred to an autoclave and heated in an oven at 160 °C for 10 h. Then the suspension was separated by centrifugation and dried. Obtained NPs had the $\text{CoO}/\text{Co}_3\text{O}_4$ structure, as proven by X-ray phase analysis [96].

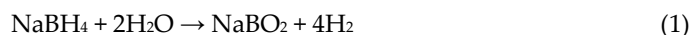
Apart from carbon foam, there are also hybrid materials based on carbon fibers and various nanoparticles, and the combinations of porous fibers and metal nanoparticles provide new unique properties. To prepare hybrid membranes from carbon nanofibers and nanoparticles of cobalt and nickel, the carbon fiber membrane was preliminarily treated with concentrated sulfuric acid for 30 min to increase its hydrophilic properties and then washed several times with deionized water. Then, the carbon fiber membrane was immersed in a solution containing cobalt nitrate, nickel nitrate, and urea in 50% ethanol, then heated to 80 °C in an oil bath for 6 h. The resulting membrane was then cleaned several times with deionized water and ethanol to remove by-products from the surface and dried at 70 °C for 24 h. Such systems can be useful in various production areas, especially in electronics [97]. Joint systems based on transition metals incorporated into the structure of carbon nanomaterials may be promising candidates as base metal catalysts. For example, unmodified cobalt oxides or reduced graphene oxides individually exhibit very low catalytic activity; a hybrid material of graphene with cobalt nanoparticles Co_3O_4 (according to XRD) showed a high activity of the oxygen reduction reaction [98].

Currently, products based on carbon nanotubes are gaining more and more popularity, as carbon substrate (nanotube) has a large surface area and can provide pathways for electron flow in an electrocatalytic system. One of the methods for such materials based on cobalt nanoparticles is described in the work of Atsushi Gabe et al. [99]. The essence of the method is the dissolution of the Co precursor (hexahydrate nitrate cobalt (II) ($\text{Co}(\text{NO}_3)_2 \cdot 6\text{H}_2\text{O}$)) in ethanol together with PVP polyvinylpyrrolidone and adding carbon nanotubes to this solution with vigorous stirring. First, the system was sonicated and mixed, and then sodium borohydride NaBH_4 or ammonia NH_4OH was added to this system and subjected to ultrasonic treatment at 0 °C in an ice bath. Then, for complete reduction of Co, the suspension was stirred for 2 h at 0 °C, followed by filtration and washing, and dried at 80 °C. In this case, cobalt nanoparticles had the Co_3O_4 structure (according to XPS data). Then, nanotubes with incorporated cobalt nanoparticles were calcined at 500 °C in an N_2 atmosphere for 1 h to remove PVP.

3. Applications of CoNPs

3.1. CoNPs in Catalysis

One of the most critical areas of application of cobalt nanoparticles is their use as a catalyst. For example, cobalt nanosystems catalyze the hydrolysis of sodium borane (1), which is a reaction to produce hydrogen, one of the environmentally friendly fuel and efficient energy carriers.



Bo Chen et al. obtained the Co/Fe₃O₄(5)C nanocomposite, which was used for hydrolysis of sodium borane. The system consists of cobalt nanoparticles, which are uniformly distributed on the surface of iron oxide nanocrystals, previously modified with a carbon layer [100]. In this work, comparative experiments were carried out on the material obtained without using cobalt nanoparticles Fe₃O₄@C. In this case, the rate of hydrogen formation was approximately equal to the reaction rate in the absence of a catalyst, which indicates the importance of the inclusion of cobalt nanoparticles in the synthesis. The nanocatalyst provides a hydrogen formation rate equal to 1403 mL·g⁻¹cat·min⁻¹. The possibility of reuse was also investigated, which showed that the rate slightly decreases with each subsequent use, which may be associated with eliminating cobalt nanoparticles from the nanocrystal surface during catalyst regeneration. The minimum hydrogen formation rate was 831.7 mL·g⁻¹cat·min⁻¹ [100]. Similar studies on the preparation of hybrid catalysts with CoNPs were carried out. The most efficient to note are nanostructured Co-Ni-B catalysts on a Cu support, which allow reaching a rate of 14,778 mL·g⁻¹min⁻¹ [101]. The XRD diffraction pattern of the NPs isolated for the catalysis experiment revealed phases of Ni and Co₃O₄.

Zhiting Gao et al. synthesized Co nanoparticles with a phase of metallic cobalt Co(0) (XRD data), incorporated into carbon materials treated with nitrogen, which were used in the processes of hydrogen production [102]. The rate of hydrogen formation when using this catalyst was 1807 mL·g⁻¹cat·min⁻¹, the stability of the catalyst is relatively low after the fifth hydrolysis cycle, and the catalyst efficiency dropped to 32.5%, which they attributed to the fact that borate particles are adsorbed on the catalyst surface after the first cycle, which can change the electronic configuration of cobalt and reduces its catalytic activity. After the fifth cycle, borate particles cover the entire catalyst surface, which changes its morphology.

Jin Wang et al. obtained cobalt nanoparticles, which contained phases of metallic cobalt, and phases of its oxides (XRD data), deposited on three-dimensional graphene oxide Co@3DGO for the use of these structures in catalysis [103]. The results showed that the rate of hydrogen formation when using Co@3DGO was 4394 mL·g⁻¹cat·min⁻¹. Furthermore, the catalyst efficiency was 70% after five hydrolysis cycles, which indicates its high potential for reuse and therefore creates a significant backlog in the use of such systems in the industry. On the other hand, Jinghua Li et al. showed a better efficiency for reuse, who proposed their catalyst based on cobalt oxide nanoparticles CoO encapsulated in graphite Co@NMGC [104]. It was found that the rate of hydrogen formation when using this catalyst was 3575 mL·g⁻¹cat·min⁻¹.

Furthermore, they found that after 20 hydrolysis cycles, the efficiency catalyst was 82.5%, which makes it preferable for reuse. Moreover, this composite exhibits unique durability, making it one of the most promising catalytic systems based on cobalt nanoparticles. There have been similar studies of cobalt nanocomposites [105–110], most of which have shown similar performance indicators and are suitable for repeated use. However, some may present obstacles due to structural deficiencies [102]. Moreover, attention should be paid to nanostructured catalysts containing several elements of metals and non-metals [101], as they show the highest results with a rate of hydrogen formation of 14,778 mL·g⁻¹cat·min⁻¹.

In addition to catalyzing the hydrolysis of sodium borane, cobalt nanoparticles are actively used to catalyze the decomposition of various dyes. Arijit Mondal et al. used cobalt nanoparticles in the presence of sodium borane to catalyze the decomposition of methylene orange (MO) [28], the combined use of cobalt nanoparticles with sodium borane showed high efficiency in the decomposition of the dye. A spectrophotometric method was used to control the decomposition process, namely, a decrease in the absorption intensity of the peak at 465 nm in the spectrum. Due to the presence of the azo-group, the dyes are colored, and the peak at 465 nm indicates the presence of an azo compound in the solution. The reduction of the azo-group to amino compounds is the reason for the disappearance of the color of the solution and a decrease in the intensity of the peak. The proposed mechanism for the decomposition of MO is the formation of sodium borohydride in aqueous systems, which is absorbed on the surface of a cobalt nanoparticle, followed by the release of hydrogen, which reduces the azo group to amines (Figure 2).

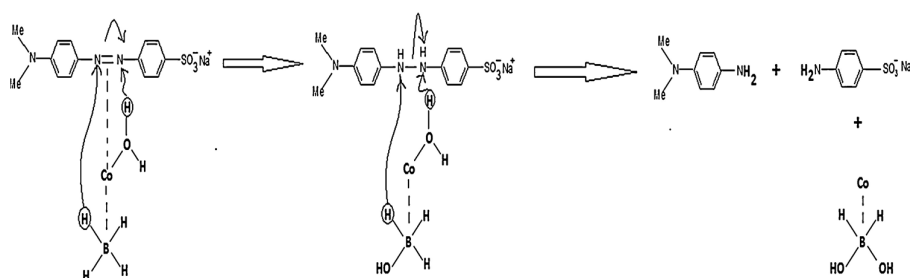


Figure 2. Mechanism of reduction of methylene orange [28].

A feature of this work is that the catalytic properties are aimed at reducing the azo-group, which is present in most organic dyes, which occupy a third of the total volume of dyes produced [28]. Furthermore, due to the magnetic properties of CoNPs, they can be separated after use from the solution with the recovered dye, regenerated, and reused. After using cobalt nanoparticles as a catalyst four times, they were reanalyzed by TEM and XRD. The result showed that the structure after their use did not change. However, the efficiency decreased markedly after the 6th use, while the rate of MO decomposition decreased by two times.

Y. Sha et al. investigated the decomposition process of Congo red, amaranth, and Orange G with cobalt nanoparticles as a catalyst [55]. Their study established a relationship between the structure of the dye, molecular weight, and the rate of degradation. The used NPs, according to the EDS results, consisted of pure metallic cobalt with an oxide layer on their surface. The decomposition rate increased with decreasing molecular weight of the dye. Deming Wu et al. conducted research on the decomposition of MO in the presence of cobalt nanoparticles Co(0), encapsulated in nanotubes, sodium bicarbonate, and sodium sulfide [111], and the time for complete decomposition of MO was increased compared with the only use of CoNPs [28]. It was 20 min (with the same amount of dye substance) at room temperature. However, the efficiency of reusing such catalysts is higher (after four cycles of using nanocomposites, the productivity decreased from 96% to 86%). The present research can help move from the laboratory to industrial processes and use this system in production.

Tahir Rasheed et al. studied the process of catalytic decomposition using cobalt oxide nanoparticles obtained by the green method from the extract of *Taraxacum officinale* [112]. Together with sodium borane, the resulting nanoparticles decomposed MO and direct yellow-142. Cobalt oxide nanoparticles also catalyze the reduction of the azo-group with an efficiency of 96%, but within 60 min, which is significantly longer than the decomposition time using the above-described catalysts. Cobalt nanoparticles obtained using green chemistry methods also exhibit catalytic activity and increase environmental friendliness and safety processes.

There are also several other experiments on the decomposition of azo dyes in the presence of other nanocatalysts [113–118]. However, using other metal nanoparticles, metal oxides, and jointly doped nanocomposites is less effective than using cobalt nanoparticles in this process since the complete disintegration of MO takes from 30 to 300 min. Furthermore, additional conditions are required to carry out this process in the absence of cobalt nanoparticles, such as UV irradiation with mercury lamps and heating. When the process is scaled up to production levels, it causes additional energy and labor costs.

C. Ravi Dhas et al. used nanoparticles of cobalt oxide Co_2O_3 (the presence of CoO and Co_2O_3 phases was revealed) as photocatalysts for the decomposition of the dyes Rhodamine B and direct red-80 [119], and the main difference from previous studies is that Rhodamine B is a cationic fluorescent dye and does not contain azo groups in its structure, a direct red-80 anionic multi-azo dye. The best photocatalytic activity in this work was shown by samples of cobalt oxide nanoparticles prepared without using a stabilizing agent; the decomposition of dyes was observed within 180 min. The maximum decomposition for Rhodamine B was 32%, for direct red-80 78%. The supposed mechanism of the degradation of the dye Rhodamine B is the photoabsorption of the catalyst initiating the formation of charged Co^{3+} particles. The formed particles transfer the charge from the catalyst to the dye, which causes the NN bond to break, which initiates the decomposition of the compound.

Dye catalysis processes are applied in various water purification systems, so M. M. El-Sayed et al. synthesized nanoporous membranes from cellulose acetate on a biological basis, poly (lactic acid), and biodegradable polyurethane impregnated with catalytic cobalt nanoparticles (Figure 3) [120] and tested their ability to remove methylene blue and Congo red from wastewater. The process was carried out under the influence of UV radiation. Wastewater dyes were adsorbed on cobalt nanoparticles in a nanoporous membrane, decomposed, and removed. Decomposition and removal efficiency was 60% for each dye. The advantage of this nanosystem is that a biopolymer carrier membrane, which is completely eco-degradable, reduces the risk of nanoparticles entering the wastewater. This work is an example of the effective use of theoretical knowledge in the field of dye catalysis, which has been successfully adapted to the production scale.

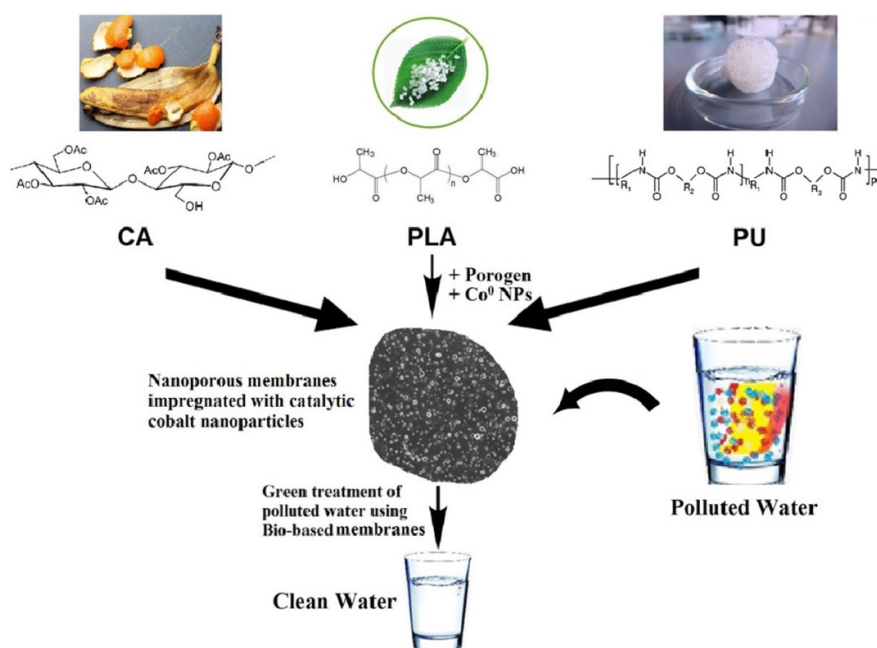


Figure 3. Nanoporous membranes synthesized from bio-based polymeric blends and impregnated with CoNPs for the treatment of polluted water [120].

Cobalt oxide nanoparticles provide a high percentage of decomposition for azo dyes, which has been shown in several studies and can catalyze the decomposition of cationic dyes. In addition, nanoparticles obtained using green methods can also catalyze degradation processes. A magnetic field or inclusion in various structures can be used to separate the nanoparticles, which suggests the possibility of using CoNPs on an industrial scale to treat industrial wastewater.

Another important application of CoNPs is in the Fischer–Tropsch process [121], the essence of which is the catalytic hydrogenation of carbon monoxide (CO) to longer chain hydrocarbons. Co catalysts are prized for their ability to produce more and longer chains. The influence of cobalt nanoparticles on the process has been studied for many years, and it was found that the size of the nanoparticles used is of great importance, with several studies showing the dependence of the size of nanoparticles on the efficiency of their catalytic properties in the Fischer–Tropsch process [122,123].

3.2. CoNPs as an Anticancer Drug

CoNPs have a high surface area, high mass transfer, and magnetic properties, making them successful agents for treating neoplastic diseases. They can be used as an effective carrier for cytotoxic drugs and toxic for tumor cells [124]. CoNPs are highly cytotoxic towards cancer cells, and studies have shown that CoNPs obtained by the green method present the activity against cancer cells [125]. The results of this experiment showed the anticancer toxicity of CoNPs obtained using the extract of *Rhamnus virgata* leaves was proved, and established the optimal concentration, which provides the desired therapeutic effect and causes the least harm to the body—the IC₅₀ values were calculated as 33.25 (HUH-7) and 11.69 (HepG2) µg/mL, respectively. One of the critical factors is the biocompatibility of nanoparticles to the human body, and the authors also studied the biocompatibility of CoNPs to erythrocytes and established the IC₅₀ value for CoNPs against erythrocytes was 4636 µg/mL, which is much higher than the toxicity for cancer cells [125].

Nanoparticles CoO/Co₃O₄ with a cubic spinel structure (XRD results) obtained using fresh leaves of young branches of *Rosmarinus officinalis* exhibited cytotoxic properties towards human cancer cells, and it was found that the IC₅₀ value for these nanoparticles is 55 µg/mL to U87 cells, which is the optimal value for cancer therapy. In addition, nanoparticles exhibit magnetic activity, which can be used for targeted therapies [126].

S. K. Verma et al. suggested a way to get nanoparticles exhibiting cytotoxic properties, as they carried out in silico analysis to assess the interaction of CoNPs and biological compounds of the body (enzymes, amino acids, etc.). They synthesized CoO nanoparticles (determined by the XPS method) with an average size of 41 nm. In addition, MTT analysis and apoptosis in HCT116 cells were performed, and the result showed that the IC₅₀ was set at 44 µg/mL for HCT116 cells. It was also found that nanoparticles produced by green methods induce less apoptosis in colon cells and zebrafish embryos than commercial cobalt nanoparticles by inducing less ROS [127]. This method shows it is possible to obtain cobalt nanoparticles using green methods and use them in cancer therapy with less harm to the body.

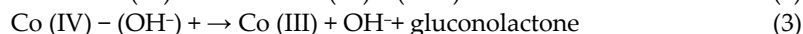
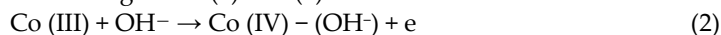
J. S. Ajarem et al. developed CoNPs by reducing the extract of red algae, exhibiting anticancer and anticoagulant activity. According to the Scherrer equation, they obtained Co₃O₄ nanoparticles (XRD results) with an average crystallite size of 26.5 nm. The present study showed a significant anticancer potential of Co₃O₄ NPs with an IC₅₀ value of 41.4 µg/mL and proved that when the Co₃O₄ NPs interact with cells, ROS is generated, which causes oxidative stress in cells, and leads to DNA damage and cell death. Results also showed that a blood clot on glass completely liquefied in 30 min; therefore, CoNPs can be actively used as a promising anticoagulant and thrombolytic agent for the therapy of thrombosis [80]. These nanoparticles have shown high efficiency in the treatment of cancer cells, as well as a promising anticoagulant. The anticoagulant activity caused by nanoparticles may be associated with the inhibition of certain enzymes that catalyze thrombin formation in the body. Due to the green method of obtaining cobalt nanoparticles, as well

as high efficiency in the fight against cancer and thrombolytic diseases, it can be stated that the particles obtained are one of the most promising nanomaterials that can soon be used in the treatment of various diseases. Nanoparticles obtained using *Euphorbia tirucalli* stem extract had a CoO structure (XPS and XRD method) and showed high efficacy against the MCF-7 line of breast cancer with $IC_{50} < 10 \mu\text{g/mL}$. This value indicates that nanoparticles exhibit high cytotoxicity to these cells, ensuring the high efficacy of anti-tumor therapy for breast cancer [128].

Given that the fundamental mechanisms occurring in the human body are critical for the treatment of tumor diseases, researchers have studied the effect of oxygen and adsorption on the surfaces of cobalt nanoparticles using DFT computational methods [129], and as a result, assessed the energy and structural parameters, and established the dipole nature of the oxygen-cobalt bond in the human body. In addition, they established the thermodynamic parameters of the system, which affected the chemical and magnetic properties of cobalt nanoparticles. They proved that for the use of nanoparticles for biomedical purposes, it is necessary to add a coating layer, which ensures the biocompatibility of the particles but does not change their magnetic properties. Furthermore, it has been proven that when CoNPs enter the bloodstream, they form a non-magnetic oxide and lose their magnetic properties.

3.3. CoNPs as a Contrast Agent and Diagnostic/Theranostic Agent

CoNPs and their products can also be used as diagnostic materials in biomedicine. Due to the size proportionate with biological objects and physico-chemical properties, nanoparticles represent a good basis for use in the diagnosis and theranostics of various diseases. Shahab Maghsoudi and Arman Mohammadi, in their work, proposed a hybrid material based on cobalt nanoparticles Co_3O_4 (XRD data) and graphene nanosheets, which can be used for glucose detection (Figure 4) [130]. On an electrode modified with a graphene/cobalt nanoparticle composite material, the following mechanism was used for electrocatalytic determination of glucose (2) and (3)



A large number of active centers on the electrode surface due to the porous and one-dimensional structure of the composite material and the increased mobility of the electrolyte through the porous structure allow the determination of glucose at a concentration of 3.5 nM. Therefore, due to its high selectivity and response rate, this material has a high potential for use in medical analysis.

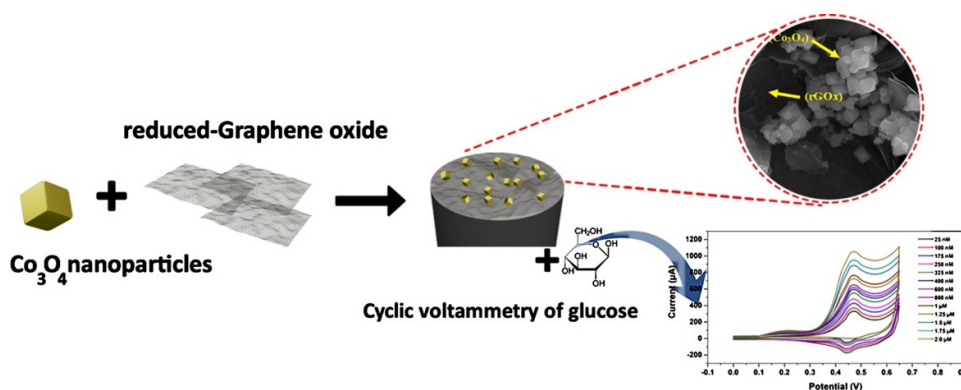


Figure 4. Biosensor for glucose detection based on the electrocatalytic reaction on rGO/ Co_3O_4 nanoparticles-modified glassy carbon electrode [130].

In their work, Q. Ren et al. proposed using manganese/cobalt oxide nanoparticles $\text{MnO}_2/\text{Co}_3\text{O}_4$ (XRD data) for theranostics of cancer [131]. Nanoparticles were obtained in three stages: 1. Preparation of cobalt nanoparticles by reduction with sodium borohydride

and stabilization with polyacrylic acid; 2. Oxidation with permanganate; 3. Rapid outward diffusion of Co forms hollow structures (Figure 5). These nanoparticles were biodegradable, which was confirmed by experiments on their incubation in phosphate-buffered saline. Due to their structure, hollow nanoparticles are an excellent carrier for various therapeutic agents, such as doxorubicin. Furthermore, during this study, it was proved that upon contact with glutathione, nanoparticles will decompose, which will lead to the release of a therapeutic drug. It has also been established that many manganese ions are released upon contact with glutathione and the decomposition of nanoparticles, which can effectively serve as a contrast agent for MRI. All the above suggests that these nanoparticles are a unique nanomaterial that can be used for several purposes for diagnostics, theranostics, and delivery of anticancer drugs, in conjunction with the controlled synthesis in the range of 10–300 nm provides a completely successful system that may soon be used in cancer theranostics.

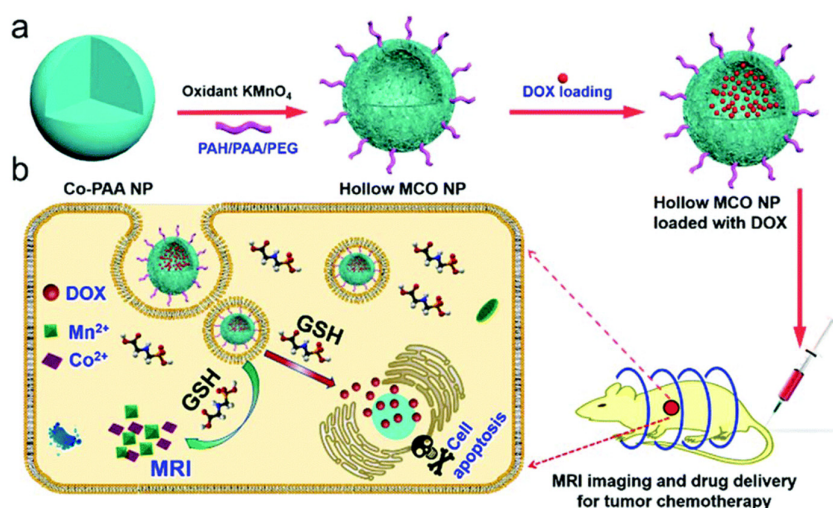


Figure 5. (a) Preparation and (b) application of CoNPs as glutathione-sensitive theranostic systems [131].

Multifunctional cobalt phosphide nanoparticles are used as contrast agents for various imaging methods for theranostics of tumor diseases and a photosensitizer in photothermal therapy (PTT) (Figure 6). At 10 min of laser irradiation, with a CoNPs concentration of $100 \mu\text{g mL}^{-1}$, the temperature rise (AT KC) was = 25.3, which is sufficient to destroy tumor cells. Infrared thermal imaging has shown that the signal intensity depends solely on the concentration and time of exposure. Cobalt phosphide nanoparticles have shown high potential as a contrast agent in photoacoustic PA tomography. Li Z. et al. demonstrated a linear relationship between the concentration of nanoparticles and the intensity of the PA signal. This method can be applied to the study of vessels in cancerous tumors and has a very high penetrating and resolving ability, which cannot be achieved with CT and MRI [132]. This work shows the high applied value of cobalt nanoparticles as an auxiliary agent for diagnostic and therapeutic purposes. Such multifunctional materials can increase the effectiveness of anticancer therapy by identifying and destroying tumors in the early stages of the disease.

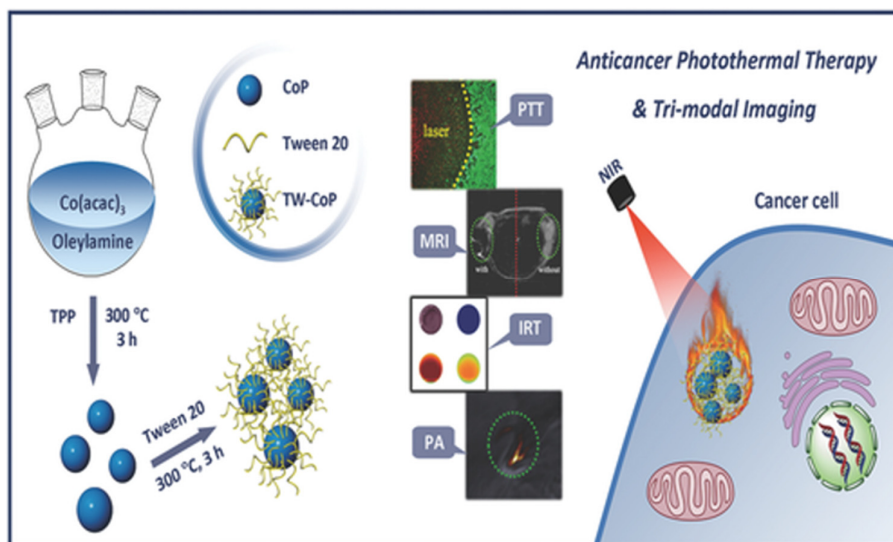


Figure 6. Synthesis and biomedical applications of CoNPs in PTT [132].

Another work demonstrating the multifunctional capabilities of cobalt nanoparticles in diagnostics is the study of Z. Li et al., who developed cobalt sulfide nanosheets modified with polyethylene glycol (NP CoS-PEG) suitable for photoacoustic/magnetic resonance imaging, as well as a photosensitizer for PTT [133]. NP CoS-PEG showed high cytotoxic activity when irradiated with 808 nm lasers for 10 min, while simply cultured cells without irradiation showed very low mortality. This fact indicates that the cytotoxic effect of nanoparticles is associated exclusively with PTT, and cells that are not exposed to laser radiation remain alive. This fact opens new possibilities and increases the focus and efficiency of photothermal therapy. In addition, NP CoS-PEG is highly effective as a contrast agent for tumor cell imaging. During the study of the tumor, mice, using MRI, which were treated with cobalt nanosheets, showed a pronounced darkening of the tissue, while the untreated remained completely light. This fact may indicate the effectiveness of cobalt nanosheets as a T2-MRI agent *in vivo*. It has also been proven that nanosheets of cobalt sulfides can be successfully used as a counter agent in photoacoustic PA tomography. A relationship was established between the concentration of nanosheets and the intensity of the PA tomography signal. In addition, intense PA signals in the mouse tumor were observed after injection of the NP CoS-PEG dispersion, in contrast to before the injection. NP CoS-PEG demonstrated high photodynamic conversion in the region of 33% and a promising bimodal diagnostic system for simultaneous PA/MR imaging, which may provide more valuable information for PTT treatment [133]. Several other studies have also shown the potential of CoNPs in theranostics [134,135] and photothermal therapy [136,137].

3.4. Magnetic Applications of CoNPs

CoNPs exhibit different magnetic properties due to their wide range of morphologies depending on the synthesis method. Various methods can be used to obtain magnetic CoNPs, and CoNPs with magnetic properties can be used in multiple areas of human life [138]. In addition, magnetic CoNPs and products based on them can be successfully used in catalysis [139–141].

Tong Liu et al. proposed a method for synthesizing Co@CoO magnetic nanoparticles, and their structure was confirmed using XRD methods. The nanoparticles developed by the authors had a crystal size of 2 to 5 nm and exhibited magnetic properties. In addition, these particles have shown themselves as absorbers of microwaves, attributed to the microporous morphology, nanosize, and core-shell structure. The obtained NPs are a promising basis for creating highly efficient microwave radiation absorbers [142].

Sayed Zia Mohammadi developed a hybrid material based on magnetic CoNPs modified with activated carbon, used for wastewater treatment. The CoNPs were obtained by co-precipitation and had a thin film structure with a thickness of 25 nm and a diameter of 50 nm, and had the structure of metallic Co(0) determined by XRD. The resulting material showed high sorption capacity to phenol, which can serve as the basis for coatings for wastewater treatment. Furthermore, Co NPs, due to their high magnetization, exhibit a higher specific power loss than, for example, iron oxide nanoparticles, which makes them interesting as potential candidates for use in wastewater treatment since adsorbents can be easily separated from the solution using a magnetic separator [143].

Mahmoud Roushani synthesized magnetic cobalt nanoparticles modified with sodium dodecyl sulfate and ligand 2-(5-bromo-2-pyridylazo)-5-diethylaminophenol using the chemical co-precipitation method. This method is easily reproducible and has a low cost, and the diameter of cobalt nanoparticles was 100 nm. The study results proved that these modified nanoparticles could be successfully used to select lead ions, which can harm the environment. It should be especially noted that due to the magnetic properties of the resulting nanoparticles, they can be easily and quickly removed from the reaction system. In addition, the authors showed the possibility of using such systems for the separation of lead ions from other ions, which can be actively used for quantitative analysis of the content of lead ions in various systems. Furthermore, it was found that such systems have a high degree of regeneration, which reduces the cost of the process and allows the reuse of cobalt nanoparticles. The modified cobalt nanoparticles also did not retain magnetization after removing the external magnetic field, which proved the superparamagnetic properties of these nanomaterials [144].

Cobalt magnetic nanoparticles are a very promising material for diagnosing and treating various diseases. For example, the heat release of these particles in an alternating current magnetic field can be used for local hyperthermia in tumor therapy.

Matthias Zeisberger obtained magnetic nanoparticles of metallic cobalt Co (determined by XRD) with a size of 10 nm or less. These nanoparticles had a high specific heating power, superior to magnetic iron oxide nanoparticles [145]

This fact makes it possible to use cobalt nanoparticles in a sufficiently low concentration for local therapy using a magnetic field. At the same time, due to the high rate of specific heating power, the effectiveness of treatment will not decrease. However, for the successful use of these samples as therapeutic agents, it is necessary to reduce the toxicity exhibited by cobalt nanoparticles.

Laura M. Parkes et al. suggest using the magnetic properties of cobalt nanoparticles as an MRI contrast agent. They compared the developed nanoparticles to iron oxide nanoparticles and noted that cobalt nanoparticles look more attractive in terms of several indicators, such as relaxation abilities. This development will increase the efficiency of diagnostics performed using magnetic resonance methods [22].

3.5. CoNPs Toxicity

In addition to beneficial therapeutic and diagnostic properties, it is necessary to understand that they will also harm the human body at this study stage of cobalt nanoparticles. Cobalt is an important metal for humans, but it has systemic toxicity, including neurological, cardiovascular, and endocrine disorders, mainly attributable to free ionic Co (II) with blood concentrations of more than 300 µg/L) assumed to cause anxiety [146]—the ability to replace iron in metalloenzymes with the formation of substituted-inert complexes. For example, the replacement of iron with cobalt in prolyl 4-hydroxylase suppresses the regular activity of the enzyme to activate transcription sensitive to hypoxia, which causes hypoxia in mammalian cells [147]. Furthermore, due to the developed surface of nanoparticles, they can adsorb various substances from biological media onto their surface. It has long been known that nanoparticles of a specific size, shape, and charge can pass the blood-brain barrier and interact with the central nervous system. This fact is sig-

nificant for the use of nanoparticles in biomedical systems. Still, the mechanisms of interaction between nanoparticles and substances in the central nervous system are very little studied due to the complexity of the processes. In their research, M. Nouri analyzed the effect of cobalt oxide nanoparticles on PC-12 cell lines and found that due to the adsorption of proteins on the developed surface of nanoparticles, the tertiary structure of tau proteins is destabilized, and causes a more compact conformation of the secondary structure [148]. Co_3O_4 NPs exhibit a cytotoxic effect against PC-12 cells, which is also an essential factor that must be considered when using these nanoparticles.

4. Conclusions

The growing interest in CoNPs has led to many complex studies on their synthesis. It is vital for researchers to develop a simple and effective method for producing cobalt nanoparticles and to study the key parameters that affect the physico-chemical properties of the resulting nanoparticles. In recent years, green chemistry methods have become increasingly relevant, significantly increasing the nanoparticle synthesis process's environmental friendliness and safety, and simplifying the scaling of processes. Cobalt nanoparticles synthesized using solution methods can undergo further modification, for example, doping with other ions to increase their activity. This review mainly focuses on the latest advances in synthesizing, modifying, and applying cobalt nanoparticles in catalysis, cancer treatment, and diagnostic materials based on CoNPs. Besides the synthesis method and applications, the review also highlights the properties of synthesized CoNPs, including their chemical formula and structure, and the methods of analysis, such as XRD, XPS, and EDX methods. To elucidate the mechanisms of education, more detailed and systematic research is required. Understanding the detailed mechanisms of nanoparticle formation requires more serious research methods, including in situ. Currently, researchers can obtain nanoparticles of various characteristics using similar methods and precursors. Recently, many studies have focused on applying cobalt nanoparticles in catalysis, biomedicine, photodynamic therapy, and as a contrast agent. Currently, there are many works devoted to the catalysis of various processes using cobalt nanoparticles. A large-scale transition from laboratory to industrial research is now required. Cobalt nanoparticles can be used as a drug carrier, allowing drugs to reach affected areas of the body while keeping healthy tissue intact. In addition, the magnetic properties can positively affect the targeting of drug delivery. Therefore, it is necessary to pay attention to developing new formulations that increase the effectiveness of substances at a minimum concentration and minimize side effects. Particular attention should be paid to using cobalt nanoparticles as a contrast agent in MRI and photoacoustic tomography, improving the comprehensive study of body tissues and diagnosing diseases with high accuracy. Cobalt nanoparticles increase the resolution of these methods and make it possible to study even the vessels of tumor tissues. It should be noted that cobalt nanoparticles obtained even by green methods exhibit high cytotoxicity, which can be used in the fight against tumor diseases. Moreover, cobalt nanoparticles have shown high efficiency as a photosensitizer for photothermal therapy, and considering the peculiarity of nanoparticles, they can first help in determining the localization of the tumor and at the same time be used for treatment. This study shows the relevance and necessity of a deep analysis of the synthesis and application of cobalt nanoparticles in various industries since not all the unique properties of nanoparticles are currently being used.

Author Contributions: Manuscript conception, A.A.V.; design of the article, A.A.V. and P.K.; literature data analysis, A.A.V. and F.Y.P.; writing—original draft preparation, A.A.V., F.Y.P. and P.K.; writing—review and editing, A.A.V., I.A.V., Y.M.S. and P.K. All authors have read and agreed to the published version of the manuscript.

Funding: This research received no external funding.

Data Availability Statement: The data presented in this study are available in article.

Acknowledgments: The publication has been prepared with the support of the «RUDN University Strategic Academic Leadership Program».

Conflicts of Interest: The authors declare no conflict of interest.

References

1. Szczypiński, F.T.; Bennett, S.; Jelfs, K.E. Can we predict materials that can be synthesised? *Chem. Sci.* **2021**, *12*, 830–840. <https://doi.org/10.1039/d0sc04321d>.
2. Fan, Z.; Zhang, Y.; Pan, L.; Ouyang, J.; Zhang, Q. Recent developments in flexible thermoelectrics: From materials to devices. *Renew. Sustain. Energy Rev.* **2021**, *137*, 110448. <https://doi.org/10.1016/j.rser.2020.110448>.
3. Nasrollahzadeh, M.; Sajjadi, M.; Irvani, S.; Varma, R.S. Green-synthesized nanocatalysts and nanomaterials for water treatment: Current challenges and future perspectives. *J. Hazard. Mater.* **2021**, *401*, 123401. <https://doi.org/10.1016/j.jhazmat.2020.123401>.
4. Manickam, S.; Ashokkumar, M. Cavitation: A Novel Energy-Efficient Technique for the Generation of Nanomaterials. In *Cavitation: A Novel Energy-Efficient Technique for the Generation of Nanomaterials*; CRC Press: Boca Raton, FL, USA, 2014; pp. 1–433. <https://doi.org/10.4032/9789814411554>.
5. Gong, N.; Sheppard, N.C.; Billingsley, M.M.; June, C.H.; Mitchell, M.J. Nanomaterials for T-cell cancer immunotherapy. *Nat. Nanotechnol.* **2021**, *16*, 25–36. <https://doi.org/10.1038/s41565-020-00822-y>.
6. Gao, X.; Li, L.; Cai, X.; Huang, Q.; Xiao, J.; Cheng, Y. Targeting nanoparticles for diagnosis and therapy of bone tumors: Opportunities and challenges. *Biomaterials* **2021**, *265*, 120404. <https://doi.org/10.1016/j.biomaterials.2020.120404>.
7. Gautam, A.; Komal, P.; Gautam, P.; Sharma, A.; Kumar, N.; Jung, J. Recent Trends in Noble Metal Nanoparticles for Colorimetric Chemical Sensing and Micro-Electronic Packaging Applications. *Metals* **2021**, *11*, 329. <https://doi.org/10.3390/met11020329>.
8. Yanat, M.; Schroën, K. Preparation methods and applications of chitosan nanoparticles; with an outlook toward reinforcement of biodegradable packaging. *React. Funct. Polym.* **2021**, *161*, 104849. <https://doi.org/10.1016/j.reactfunctpolym.2021.104849>.
9. Dawood, M.A.O.; El Basuini, M.F.; Yilmaz, S.; Abdel-Latif, H.M.R.; Kari, Z.A.; Razab, M.K.A.A.; Ahmed, H.A.; Alagawany, M.; Gewaily, M.S. Selenium Nanoparticles as a Natural Antioxidant and Metabolic Regulator in Aquaculture: A Review. *Antioxidants* **2021**, *10*, 1364. <https://doi.org/10.3390/antiox10091364>.
10. Rashki, S.; Asgarpour, K.; Tarrahimofrad, H.; Hashemipour, M.; Ebrahimi, M.S.; Fathizadeh, H.; Khorshidi, A.; Khan, H.; Marzhooseyni, Z.; Salavati-Niasari, M.; et al. Chitosan-based nanoparticles against bacterial infections. *Carbohydr. Polym.* **2021**, *251*, 117108. <https://doi.org/10.1016/j.carbpol.2020.117108>.
11. Montes-García, V.; Squillaci, M.A.; Diez-Castellnou, M.; Ong, Q.K.; Stellacci, F.; Samori, P. Chemical sensing with Au and Ag nanoparticles. *Chem. Soc. Rev.* **2020**, *50*, 1269–1304. <https://doi.org/10.1039/d0cs01112f>.
12. Yang, W.; Pan, M.; Huang, C.; Zhao, Z.; Wang, J.; Zeng, H. Graphene oxide-based noble-metal nanoparticles composites for environmental application. *Compos. Commun.* **2021**, *24*, 100645. <https://doi.org/10.1016/j.coco.2021.100645>.
13. Vodyashkin, A.A.; Rizk, M.G.H.; Kezimana, P.; Kirichuk, A.A.; Stanishevskiy, Y.M. Application of Gold Nanoparticle-Based Materials in Cancer Therapy and Diagnostics. *ChemEngineering* **2021**, *5*, 69. <https://doi.org/10.3390/chemengineering5040069>.
14. Yaqoob, A.A.; Umar, K.; Ibrahim, M.N.M. Silver nanoparticles: Various methods of synthesis, size affecting factors and their potential applications—A review. *Appl. Nanosci.* **2020**, *10*, 1369–1378. <https://doi.org/10.1007/s13204-020-01318-w>.
15. Zan, Y.; Salmon, L.; Bousseksou, A. Morphological Studies of Composite Spin Crossover@SiO₂ Nanoparticles. *Nanomaterials* **2021**, *11*, 3169. <https://doi.org/10.3390/nano11123169>.
16. Dolara, P. Occurrence, exposure, effects, recommended intake and possible dietary use of selected trace compounds (aluminium, bismuth, cobalt, gold, lithium, nickel, silver). *Int. J. Food Sci. Nutr.* **2014**, *65*, 911–924. <https://doi.org/10.3109/09637486.2014.937801>.
17. Debussche, L.; Couder, M.; Thibaut, D.; Cameron, B.; Crouzet, J.; Blanche, F. Assay, purification, and characterization of cobaltochelatase, a unique complex enzyme catalyzing cobalt insertion in hydrogenobyrinic acid a,c-diamide during coenzyme B12 biosynthesis in *Pseudomonas denitrificans*. *J. Bacteriol.* **1992**, *174*, 7445–7451. <https://doi.org/10.1128/jb.174.22.7445-7451.1992>.
18. Neil, E.; Marsh, E.N. Coenzyme B12 (cobalamin)-dependent enzymes. *Essays Biochem.* **1999**, *34*, 139–154. <https://doi.org/10.1042/bse0340139>.
19. Dong, H.; Meininger, A.; Jiang, H.; Moon, K.-S.; Wong, C.P. Magnetic Nanocomposite for Potential Ultrahigh Frequency Microelectronic Application. *J. Electron. Mater.* **2007**, *36*, 593–597. <https://doi.org/10.1007/s11664-007-0112-x>.
20. Jarestan, M.; Khalatbari, K.; Pouraei, A.; Shandiz, S.A.S.; Beigi, S.; Hedayati, M.; Majlesi, A.; Akbari, F.; Salehzadeh, A. Preparation, characterization, and anticancer efficacy of novel cobalt oxide nanoparticles conjugated with thiosemicarbazide. *3 Biotech* **2020**, *10*, 1–9. <https://doi.org/10.1007/s13205-020-02230-4>.
21. Pucho, M.; Liu, L.; Concepción, P.; Sorribes, I.; Corma, A. Tuning the Catalytic Performance of Cobalt Nanoparticles by Tungsten Doping for Efficient and Selective Hydrogenation of Quinolines under Mild Conditions. *ACS Catal.* **2021**, *11*, 8197–8210. <https://doi.org/10.1021/acscatal.1c01561>.
22. Parkes, L.M.; Hodgson, R.; Lu, L.T.; Tung, L.D.; Robinson, I.; Fernig, D.G.; Thanh, N.T.K. Cobalt nanoparticles as a novel magnetic resonance contrast agent-relaxivities at 1.5 and 3 Tesla. *Contrast Media Mol. Imaging* **2008**, *3*, 150–156. <https://doi.org/10.1002/cmim.241>.
23. Farkaš, B.; Terranova, U.; De Leeuw, N.H. The mechanism underlying the functionalisation of cobalt nanoparticles by carboxylic acids: A first-principles computational study. *J. Mater. Chem. B* **2021**, *9*, 4915–4928. <https://doi.org/10.1039/d0tb02928a>.

24. De, D.; Upadhyay, P.; Das, A.; Ghosh, A.; Adhikary, A.; Goswami, M.M. Studies on cancer cell death through delivery of dopamine as anti-cancer drug by a newly functionalized cobalt ferrite nano-carrier. *Colloids Surfaces A Physicochem. Eng. Asp.* **2021**, *627*, 127202. <https://doi.org/10.1016/j.colsurfa.2021.127202>.
25. Jincy, C.; Meena, P. Synthesis, characterization, and NH₃ gas sensing application of Zn doped cobalt oxide nanoparticles. *Inorg. Chem. Commun.* **2020**, *120*, 108145. <https://doi.org/10.1016/j.inoche.2020.108145>.
26. Iravani, S.; Varma, R.S. Sustainable synthesis of cobalt and cobalt oxide nanoparticles and their catalytic and biomedical applications. *Green Chem.* **2020**, *22*, 2643–2661. <https://doi.org/10.1039/d0gc00885k>.
27. Haq, S.; Abbasi, F.; Ben Ali, M.; Hedfi, A.; Mezni, A.; Rehman, W.; Waseem, M.; Khan, A.R.; Shaheen, H. Green synthesis of cobalt oxide nanoparticles and the effect of annealing temperature on their physicochemical and biological properties. *Mater. Res. Express* **2021**, *8*, 075009. <https://doi.org/10.1088/2053-1591/ac1187>.
28. Mondal, A.; Adhikary, B.; Mukherjee, D. Room-temperature synthesis of air stable cobalt nanoparticles and their use as catalyst for methyl orange dye degradation. *Colloids Surfaces A Physicochem. Eng. Asp.* **2015**, *482*, 248–257. <https://doi.org/10.1016/j.colsurfa.2015.05.011>.
29. Liang, X.; Zhao, L. Room-temperature synthesis of air-stable cobalt nanoparticles and their highly efficient adsorption ability for Congo red. *RSC Adv.* **2012**, *2*, 5485–5487. <https://doi.org/10.1039/c2ra20240a>.
30. Clifford, D.; El-Gendy, A.A.; Lu, A.J.; Pestov, D.; Carpenter, E.E. Room Temperature Synthesis of Highly Magnetic Cobalt Nanoparticles by Continuous Flow in a Microfluidic Reactor. *J. Flow Chem.* **2014**, *4*, 148–152. <https://doi.org/10.1556/jfc-d-14-00013>.
31. Guo, F.; Zheng, H.; Yang, Z.; Qian, Y. Synthesis of cobalt nanoparticles in ethanol hydrazine alkaline system (EHAS) at room temperature. *Mater. Lett.* **2002**, *56*, 906–909. [https://doi.org/10.1016/s0167-577x\(02\)00635-3](https://doi.org/10.1016/s0167-577x(02)00635-3).
32. Zola, A.S.; Ribeiro, R.U.; Bueno, J.M.; Zanchet, D.; Arroyo, P. Cobalt nanoparticles prepared by three different methods. *J. Exp. Nanosci.* **2012**, *9*, 398–405. <https://doi.org/10.1080/17458080.2012.662723>.
33. Ansari, S.; Bhor, R.; Pai, K.; Sen, D.; Mazumder, S.; Ghosh, K.; Kolekar, Y.; Ramana, C. Cobalt nanoparticles for biomedical applications: Facile synthesis, physicochemical characterization, cytotoxicity behavior and biocompatibility. *Appl. Surf. Sci.* **2017**, *414*, 171–187. <https://doi.org/10.1016/j.apsusc.2017.03.002>.
34. Seong, G.; Takami, S.; Arita, T.; Minami, K.; Hojo, D.; Yavari, A.R.; Adschiri, T. Supercritical hydrothermal synthesis of metallic cobalt nanoparticles and its thermodynamic analysis. *J. Supercrit. Fluids* **2011**, *60*, 113–120. <https://doi.org/10.1016/j.supflu.2011.05.003>.
35. Kim, M.; Son, W.-S.; Ahn, K.H.; Kim, D.S.; Lee, H.-S.; Lee, Y.-W. Hydrothermal synthesis of metal nanoparticles using glycerol as a reducing agent. *J. Supercrit. Fluids* **2014**, *90*, 53–59. <https://doi.org/10.1016/j.supflu.2014.02.022>.
36. Liu, X.; Qiu, G.; Li, X. Shape-controlled synthesis and properties of uniform spinel cobalt oxide nanocubes. *Nanotechnology* **2005**, *16*, 3035–3040. <https://doi.org/10.1088/0957-4484/16/12/051>.
37. Xie, B.; Qian, Y.; Zhang, S.; Fu, S.; Yu, W. A Hydrothermal Reduction Route to Single-Crystalline Hexagonal Cobalt Nanowires. *Eur. J. Inorg. Chem.* **2006**, *2006*, 2454–2459. <https://doi.org/10.1002/ejic.200600061>.
38. Alagiri, M.; Muthamizhchelvan, C.; Hamid, S.B.A. Synthesis of superparamagnetic cobalt nanoparticles through solvothermal process. *J. Mater. Sci. Mater. Electron.* **2013**, *24*, 4157–4160. <https://doi.org/10.1007/s10854-013-1375-z>.
39. Xu, R.; Xie, T.; Zhao, Y.; Li, Y. Quasi-homogeneous catalytic hydrogenation over monodisperse nickel and cobalt nanoparticles. *Nanotechnology* **2007**, *18*, 55602. <https://doi.org/10.1088/0957-4484/18/5/055602>.
40. Shin, N.C.; Lee, Y.-H.; Shin, Y.H.; Kim, J.; Lee, Y.-W. Synthesis of cobalt nanoparticles in supercritical methanol. *Mater. Chem. Phys.* **2010**, *124*, 140–144. <https://doi.org/10.1016/j.matchemphys.2010.06.005>.
41. Dumestre, F.; Chaudret, B.; Amiens, C.; Fromen, M.-C.; Casanove, M.-J.; Renaud, P.; Zurcher, P. Shape Control of Thermodynamically Stable Cobalt Nanorods through Organometallic Chemistry. *Angew. Chem. Int. Ed.* **2002**, *41*, 4286–4289. [https://doi.org/10.1002/1521-3773\(20021115\)41:223.0.co;2-m](https://doi.org/10.1002/1521-3773(20021115)41:223.0.co;2-m).
42. Zhang, Z.; Chen, X.; Zhang, X.; Shi, C. Synthesis and magnetic properties of nickel and cobalt nanoparticles obtained in DMF solution. *Solid State Commun.* **2006**, *139*, 403–405. <https://doi.org/10.1016/j.ssc.2006.06.040>.
43. Osuna, J.; de Caro, D.; Amiens, C.; Chaudret, B.; Snoeck, E.; Respaud, M.; Broto, J.-M.; Fert, A. Synthesis, Characterization, and Magnetic Properties of Cobalt Nanoparticles from an Organometallic Precursor. *J. Phys. Chem.* **1996**, *100*, 14571–14574. <https://doi.org/10.1021/jp961086e>.
44. Scariot, M.; Silva, D.O.; Scholten, J.D.; Machado, G.; Teixeira, S.R.; Novak, M.A.; Ebeling, G.; Dupont, J. Cobalt Nanocubes in Ionic Liquids: Synthesis and Properties. *Angew. Chem. Int. Ed.* **2008**, *47*, 9075–9078. <https://doi.org/10.1002/anie.200804200>.
45. Verma, M.; Mitan, M.; Kim, H.; Vaya, D. Efficient photocatalytic degradation of Malachite green dye using facilely synthesized cobalt oxide nanomaterials using citric acid and oleic acid. *J. Phys. Chem. Solids* **2021**, *155*, 110125. <https://doi.org/10.1016/j.jpcs.2021.110125>.
46. Nam, K.M.; Shim, J.H.; Ki, H.; Choi, S.-I.; Lee, G.; Jang, J.K.; Jo, Y.; Jung, M.-H.; Song, H.; Park, J.T. Single-Crystalline Hollow Face-Centered-Cubic Cobalt Nanoparticles from Solid Face-Centered-Cubic Cobalt Oxide Nanoparticles. *Angew. Chem. Int. Ed.* **2008**, *47*, 9504–9508. <https://doi.org/10.1002/anie.200803048>.
47. Song, Y.; Henry, L.L.; Yang, W. Stable Amorphous Cobalt Nanoparticles Formed by an in Situ Rapidly Cooling Microfluidic Process. *Langmuir* **2009**, *25*, 10209–10217. <https://doi.org/10.1021/la9009866>.
48. Salman, S.A.; Usami, T.; Kuroda, K.; Okido, M. Synthesis and Characterization of Cobalt Nanoparticles Using Hydrazine and Citric Acid. *J. Nanotechnol.* **2014**, *2014*, 1–6. <https://doi.org/10.1155/2014/525193>.
49. Cruz, J.C.; Nascimento, M.A.; Amaral, H.A.; Lima, D.S.; Teixeira, A.P.C.; Lopes, R.P. Synthesis and characterization of cobalt nanoparticles for application in the removal of textile dye. *J. Environ. Manag.* **2019**, *242*, 220–228. <https://doi.org/10.1016/j.jenvman.2019.04.059>.

50. Song, Y.; Modrow, H.; Henry, L.L.; Saw, C.K.; Doomes, E.E.; Palshin, V.; Hormes, A.J.; Kumar, C.S.S.R.; Bonn, D. Microfluidic Synthesis of Cobalt Nanoparticles. *Chem. Mater.* **2006**, *18*, 2817–2827. <https://doi.org/10.1021/cm052811d>.
51. Duggan, J.N.; Bozack, M.J.; Roberts, C.B. The synthesis and arrested oxidation of amorphous cobalt nanoparticles using DMSO as a functional solvent. *J. Nanopart. Res.* **2013**, *15*, 1–16. <https://doi.org/10.1007/s11051-013-2089-0>.
52. Balela, M.D.L.; Yagi, S.; Matsubara, E. Room-Temperature Synthesis of Cobalt Nanoparticles by Electroless Deposition in Aqueous Solution. *Electrochem. Solid-State Lett.* **2010**, *13*, D4–D6. <https://doi.org/10.1149/1.3265525>.
53. Li, H.; Liao, S. Organic colloid method to prepare ultrafine cobalt nanoparticles with the size of 2 nm. *Solid State Commun.* **2008**, *145*, 118–121. <https://doi.org/10.1016/j.ssc.2007.10.014>.
54. Yanilkin, V.V.; Nasretidnova, G.R.; Osin, Y.; Salnikov, V.V. Anthracene mediated electrochemical synthesis of metallic cobalt nanoparticles in solution. *Electrochim. Acta* **2015**, *168*, 82–88. <https://doi.org/10.1016/j.electacta.2015.03.214>.
55. Sha, Y.; Mathew, I.; Cui, Q.; Clay, M.; Gao, F.; Zhang, X.J.; Gu, Z. Rapid degradation of azo dye methyl orange using hollow cobalt nanoparticles. *Chemosphere* **2016**, *144*, 1530–1535. <https://doi.org/10.1016/j.chemosphere.2015.10.040>.
56. Kim, H.-G.; Lee, H.; Kim, B.H.; Kim, S.-J.; Lee, J.-M.; Jung, S.-C. Synthesis Process of Cobalt Nanoparticles in Liquid-Phase Plasma. *Jpn. J. Appl. Phys.* **2013**, *52*, 01AN03. <https://doi.org/10.7567/jjap.52.01an03>.
57. Sergiienko, R.; Shibata, E.; Zentaro, A.; Shindo, D.; Nakamura, T.; Qin, G. Formation and characterization of graphite-encapsulated cobalt nanoparticles synthesized by electric discharge in an ultrasonic cavitation field of liquid ethanol. *Acta Mater.* **2007**, *55*, 3671–3680. <https://doi.org/10.1016/j.actamat.2007.02.017>.
58. Арефьева, Л.; Кравцов, А.; Блинов, А.; Харченко, С.; Серов, А.; Соловьев, И. Synthesis and Investigation of Cobalt Containing Nanoparticles Morphology. *Her. Bauman Mosc. State Tech. Univ. Ser. Nat. Sci.* **2017**, *71*, 85–95. <https://doi.org/10.18698/1812-3368-2017-2-85-95>.
59. Sun, S.; Murray, C.B. Synthesis of monodisperse cobalt nanocrystals and their assembly into magnetic superlattices (invited). *J. Appl. Phys.* **1999**, *85*, 4325–4330. <https://doi.org/10.1063/1.370357>.
60. Khusnuriyalova, A.F.; Caporali, M.; Hey-Hawkins, E.; Sinyashin, O.G.; Yakhvarov, D.G. Preparation of Cobalt Nanoparticles. *Eur. J. Inorg. Chem.* **2021**, *2021*, 3023–3047. <https://doi.org/10.1002/ejic.202100367>.
61. Salavati-Niasari, M.; Davar, F.; Mazaheri, M.; Shaterian, M. Preparation of cobalt nanoparticles from [bis(salicylidene)cobalt(II)]-oleylamine complex by thermal decomposition. *J. Magn. Magn. Mater.* **2008**, *320*, 575–578. <https://doi.org/10.1016/j.jmmm.2007.07.020>.
62. Hertrich, M.F.; Schamagl, F.K.; Pews-Davtyan, A.; Kreyenschulte, C.R.; Lund, H.; Bartling, S.; Jackstell, R.; Beller, M. Supported Cobalt Nanoparticles for Hydroformylation Reactions. *Chem.—A Eur. J.* **2019**, *25*, 5534–5538. <https://doi.org/10.1002/chem.201806282>.
63. Malik, M.A.; Wani, M.Y.; Hashim, M.A. Microemulsion method: A novel route to synthesize organic and inorganic nanomaterials. *Arab. J. Chem.* **2012**, *5*, 397–417. <https://doi.org/10.1016/j.arabj.2010.09.027>.
64. Das, A.; Natarajan, K.; Tiwari, S.; Ganguli, A.K. Nanostructures synthesized by the reverse microemulsion method and their magnetic properties. *Mater. Res. Express* **2020**, *7*, 7. <https://doi.org/10.1088/2053-1591/abbb55>.
65. Li, J.; Li, X.; Liang, D.; Zhang, X.; Lin, Q.; Hao, L. Preparation and Antibacterial Performances of Electrocatalytic Zinc Oxide Nanoparticles with Diverse Morphologies. *J. Biomed. Nanotechnol.* **2021**, *17*, 1824–1829. <https://doi.org/10.1166/jbn.2021.3144>.
66. Haq, S.; Ahmad, P.; Khandaker, M.U.; Faruque, M.R.I.; Rehman, W.; Waseem, M.; Din, S.U. Antibacterial, antioxidant and physico-chemical investigations of tin dioxide nanoparticles synthesized via microemulsion method. *Mater. Res. Express* **2021**, *8*, 035013. <https://doi.org/10.1088/2053-1591/abed8a>.
67. Bezza, F.A.; Tichapondwa, S.M.; Chirwa, E.M.N. Fabrication of monodispersed copper oxide nanoparticles with potential application as antimicrobial agents. *Sci. Rep.* **2020**, *10*, 1–18. <https://doi.org/10.1038/s41598-020-73497-z>.
68. Kale, A.R.; Barai, D.P.; Bhanvase, B.A.; Sonawane, S.H. An Ultrasound-Assisted Minireactor System for Continuous Production of TiO₂ Nanoparticles in a Water-in-Oil Emulsion. *Ind. Eng. Chem. Res.* **2021**, *60*, 14747–14757. <https://doi.org/10.1021/acs.iecr.1c02413>.
69. Sopoušek, J.; Pinkas, J.; Buršík, J.; Svoboda, M.; Krásenský, P. Continuous Flow Synthesis of Iron Oxide Nanoparticles Using Water-in-Oil Microemulsion. *Colloid J.* **2020**, *82*, 727–734. <https://doi.org/10.1134/s1061933x20060174>.
70. Zhang, Y.; Chen, X.; Zhu, B.; Zhou, Y.; Liu, X.; Yang, C. Temperature-Switchable Surfactant-Free Microemulsion. *Langmuir* **2020**, *36*, 7356–7364. <https://doi.org/10.1021/acs.langmuir.0c00828>.
71. Sandhu, R.K.; Kaur, A.; Kaur, P.; Rajput, J.K.; Khullar, P.; Bakshi, M.S. Solubilization of surfactant stabilized gold nanoparticles in oil-in-water and water-in-oil microemulsions. *J. Mol. Liq.* **2021**, *336*, 116305. <https://doi.org/10.1016/j.molliq.2021.116305>.
72. Kamal, S.K.; Sahoo, P.; Premkumar, M.; Rao, N.R.; Kumar, T.J.; Sreedhar, B.; Singh, A.; Ram, S.; Sekhar, K.C. Synthesis of cobalt nanoparticles by a modified polyol process using cobalt hydrazine complex. *J. Alloys Compd.* **2009**, *474*, 214–218. <https://doi.org/10.1016/j.jallcom.2008.06.160>.
73. Khan, J.; Ullah, H.; Sajjad, M.; Ali, A.; Thebo, K.H. Synthesis, characterization and electrochemical performance of cobalt fluoride nanoparticles by reverse micro-emulsion method. *Inorg. Chem. Commun.* **2018**, *98*, 132–140. <https://doi.org/10.1016/j.inoche.2018.10.018>.
74. Meydan, E.; Demirci, S.; Aktaş, N.; Sahiner, N.; Ozturk, O.F. Boron-containing magnetic nanoparticles from Co, Ni, and Fe chloride salts and their catalytic performances on 4-nitrophenol reduction. *Inorg. Chem. Commun.* **2020**, *116*, 107930. <https://doi.org/10.1016/j.inoche.2020.107930>.
75. Nilavukkarasi, M.; Vijayakumar, S.; Kumar, S.P. Biological synthesis and characterization of silver nanoparticles with Capparis zeylanica L. leaf extract for potent antimicrobial and anti proliferation efficiency. *Mater. Sci. Energy Technol.* **2020**, *3*, 371–376. <https://doi.org/10.1016/j.mset.2020.02.008>.

76. Maheshwaran, G.; Bharathi, A.N.; Selvi, M.M.; Kumar, M.K.; Kumar, R.M.; Sudhakar, S. Green synthesis of Silver oxide nanoparticles using Zephyranthes Rosea flower extract and evaluation of biological activities. *J. Environ. Chem. Eng.* **2020**, *8*, 104137. <https://doi.org/10.1016/j.jece.2020.104137>.
77. Paiva-Santos, A.C.; Herdade, A.M.; Guerra, C.; Peixoto, D.; Pereira-Silva, M.; Zeinali, M.; Mascarenhas-Melo, F.; Paranhos, A.; Veiga, F. Plant-mediated green synthesis of metal-based nanoparticles for dermatopharmaceutical and cosmetic applications. *Int. J. Pharm.* **2021**, *597*, 120311. <https://doi.org/10.1016/j.ijpharm.2021.120311>.
78. Esa, Y.A.M.; Sapawe, N. A short review on biosynthesis of cobalt metal nanoparticles. *Mater. Today Proc.* **2020**, *31*, 378–385. <https://doi.org/10.1016/j.matpr.2020.07.183>.
79. Samuel, M.S.; Selvarajan, E.; Mathimani, T.; Santhanam, N.; Phuong, T.N.; Brindhadevi, K.; Pugazhendhi, A. Green synthesis of cobalt-oxide nanoparticle using jumbo Muscadine (*Vitis rotundifolia*): Characterization and photo-catalytic activity of acid Blue-J. *Photochem. Photobiol. B Biol.* **2020**, *211*, 112011. <https://doi.org/10.1016/j.jphotobiol.2020.112011>.
80. Ajarem, J.S.; Maooda, S.N.; Allam, A.A.; Taher, M.M.; Khalaf, M. Benign Synthesis of Cobalt Oxide Nanoparticles Containing Red Algae Extract: Antioxidant, Antimicrobial, Anticancer, and Anticoagulant Activity. *J. Clust. Sci.* **2021**, 1–12. <https://doi.org/10.1007/s10876-021-02004-9>.
81. Bibi, I.; Nazar, N.; Iqbal, M.; Kamal, S.; Nawaz, H.; Nouren, S.; Safa, Y.; Jilani, K.; Sultan, M.; Ata, S.; et al. Green and eco-friendly synthesis of cobalt-oxide nanoparticle: Characterization and photo-catalytic activity. *Adv. Powder Technol.* **2017**, *28*, 2035–2043. <https://doi.org/10.1016/j.apt.2017.05.008>.
82. Jang, E.; Ryu, B.H.; Shim, H.-W.; Ju, H.; Kim, D.-W.; Kim, T.D. Adsorption of microbial esterases on Bacillus subtilis-templated cobalt oxide nanoparticles. *Int. J. Biol. Macromol.* **2014**, *65*, 188–192. <https://doi.org/10.1016/j.ijbiomac.2014.01.027>.
83. Vijayanandan, A.S.; Balakrishnan, R.M. Biosynthesis of cobalt oxide nanoparticles using endophytic fungus Aspergillus nidulans. *J. Environ. Manag.* **2018**, *218*, 442–450. <https://doi.org/10.1016/j.jenvman.2018.04.032>.
84. Omran, B.A.; Nassar, H.; AliYounis, S.; El-Salamony, R.A.; Fatthallah, N.A.; Hamdy, A.; El-Shatoury, E.H.; El-Gendy, N.S. Novel mycosynthesis of cobalt oxide nanoparticles using Aspergillus brasiliensis ATCC 16404—Optimization, characterization and antimicrobial activity. *J. Appl. Microbiol.* **2019**, *128*, 438–457. <https://doi.org/10.1111/jam.14498>.
85. Huang, H.; Wang, J.; Zhang, J.; Cai, J.; Pi, J.; Xu, J.-F. Inspirations of Cobalt Oxide Nanoparticle Based Anticancer Therapeutics. *Pharmaceutics* **2021**, *13*, 1599. <https://doi.org/10.3390/pharmaceutics13101599>.
86. Singh, P.K.; Kumar, P.; Das, A.K. Unconventional Physical Methods for Synthesis of Metal and Non-metal Nanoparticles: A Review. *Proc. Natl. Acad. Sci. USA* **2018**, *89*, 199–221.
87. Dong, X.; Choi, C.; Kim, B. Chemical synthesis of Co nanoparticles by chemical vapor condensation. *Scr. Mater.* **2002**, *47*, 857–861. [https://doi.org/10.1016/s1359-6462\(02\)00304-4](https://doi.org/10.1016/s1359-6462(02)00304-4).
88. Wang, Z.; Choi, C.; Kim, B.; Kim, J.; Zhang, Z. Characterization and magnetic properties of carbon-coated cobalt nanocapsules synthesized by the chemical vapor-condensation process. *Carbon* **2003**, *41*, 1751–1758. [https://doi.org/10.1016/s0008-6223\(03\)00127-1](https://doi.org/10.1016/s0008-6223(03)00127-1).
89. Choi, C.; Dong, X.; Kim, B. Characterization of Fe and Co nanoparticles synthesized by chemical vapor condensation. *Scr. Mater.* **2001**, *44*, 2225–2229. [https://doi.org/10.1016/s1359-6462\(01\)00750-3](https://doi.org/10.1016/s1359-6462(01)00750-3).
90. Meng, H.; Zhao, F.; Zhang, Z. Preparation of cobalt nanoparticles by direct current arc plasma evaporation method. *Int. J. Refract. Met. Hard Mater.* **2012**, *31*, 224–229. <https://doi.org/10.1016/j.ijrmhm.2011.11.007>.
91. Song, S.; Zhou, X.; Li, L.; Ma, W. Numerical simulation and experimental validation of SiC nanoparticle distribution in magnesium melts during ultrasonic cavitation based processing of magnesium matrix nanocomposites. *Ultrason. Sonochem.* **2015**, *24*, 43–54. <https://doi.org/10.1016/j.ultsonch.2014.12.010>.
92. Ohayon, E.; Gedanken, A. The application of ultrasound radiation to the synthesis of nanocrystalline metal oxide in a non-aqueous solvent. *Ultrason. Sonochem.* **2010**, *17*, 173–178. <https://doi.org/10.1016/j.ultsonch.2009.05.015>.
93. Li, Z.; Zhuang, T.; Dong, J.; Wang, L.; Xia, J.; Wang, H.; Cui, X.; Wang, Z. Sonochemical fabrication of inorganic nanoparticles for applications in catalysis. *Ultrason. Sonochem.* **2021**, *71*, 105384. <https://doi.org/10.1016/j.ultsonch.2020.105384>.
94. Dabalà, M.; Pollet, B.G.; Zin, V.; Campadello, E.; Mason, T.J. Sonoelectrochemical (20 kHz) production of Co₆₅Fe₃₅ alloy nanoparticles from Aotani solutions. *J. Appl. Electrochem.* **2008**, *38*, 395–402. <https://doi.org/10.1007/s10800-007-9450-x>.
95. Zhang, X.; Chan, K.-Y. Microemulsion synthesis and electrocatalytic properties of platinum–cobalt nanoparticles. *J. Mater. Chem.* **2002**, *12*, 1203–1206. <https://doi.org/10.1039/b109223e>.
96. Li, X.; Li, X.; Dong, Y.; Wang, L.; Jin, C.; Zhou, N.; Chen, M.; Dong, Y.; Xie, Z.; Zhang, C. Porous cobalt oxides/carbon foam hybrid materials for high supercapacitive performance. *J. Colloid Interface Sci.* **2019**, *542*, 102–111. <https://doi.org/10.1016/j.jcis.2019.01.128>.
97. Lai, F.; Huang, Y.; Miao, Y.-E.; Liu, T. Controllable preparation of multi-dimensional hybrid materials of nickel-cobalt layered double hydroxide nanorods/nanosheets on electrospun carbon nanofibers for high-performance supercapacitors. *Electrochim. Acta* **2015**, *174*, 456–463. <https://doi.org/10.1016/j.electacta.2015.06.031>.
98. Liang, Y.; Li, Y.; Wang, H.; Zhou, J.; Wang, J.; Regier, T.; Dai, H. Co₃O₄ nanocrystals on graphene as a synergistic catalyst for oxygen reduction reaction. *Nat. Mater.* **2011**, *10*, 780–786. <https://doi.org/10.1038/nmat3087>.
99. Gabe, A.; García-Aguilar, J.; Berenguer-Murcia, Á.; Morallón, E.; Cazorla-Amorós, D. Key factors improving oxygen reduction reaction activity in cobalt nanoparticles modified carbon nanotubes. *Appl. Catal. B Environ.* **2017**, *217*, 303–312. <https://doi.org/10.1016/j.apcatb.2017.05.096>.
100. Chen, B.; Chen, S.; Bandal, H.A.; Appiah-Ntiamoah, R.; Jadhav, A.R.; Kim, H. Cobalt nanoparticles supported on magnetic core-shell structured carbon as a highly efficient catalyst for hydrogen generation from NaBH₄ hydrolysis. *Int. J. Hydrogen Energy* **2018**, *43*, 9296–9306. <https://doi.org/10.1016/j.ijhydene.2018.03.193>.

101. Wei, Y.; Meng, W.; Wang, Y.; Gao, Y.; Qi, K.; Zhang, K. Fast hydrogen generation from NaBH₄ hydrolysis catalyzed by nanostructured Co–Ni–B catalysts. *Int. J. Hydrogen Energy* **2017**, *42*, 6072–6079. <https://doi.org/10.1016/j.ijhydene.2016.11.134>.
102. Gao, Z.; Ding, C.; Wang, J.; Ding, G.; Xue, Y.; Zhang, Y.; Zhang, K.; Liu, P.; Gao, X. Cobalt nanoparticles packaged into nitrogen-doped porous carbon derived from metal-organic framework nanocrystals for hydrogen production by hydrolysis of sodium borohydride. *Int. J. Hydrogen Energy* **2019**, *44*, 8365–8375. <https://doi.org/10.1016/j.ijhydene.2019.02.008>.
103. Wang, J.; Ke, D.; Li, Y.; Zhang, H.; Wang, C.; Zhao, X.; Yuan, Y.; Han, S. Efficient hydrolysis of alkaline sodium borohydride catalyzed by cobalt nanoparticles supported on three-dimensional graphene oxide. *Mater. Res. Bull.* **2017**, *95*, 204–210. <https://doi.org/10.1016/j.materresbull.2017.07.039>.
104. Li, J.; Hong, X.; Wang, Y.; Luo, Y.; Huang, P.; Li, B.; Zhang, K.; Zou, Y.; Sun, L.; Xu, F.; et al. Encapsulated cobalt nanoparticles as a recoverable catalyst for the hydrolysis of sodium borohydride. *Energy Storage Mater.* **2020**, *27*, 187–197. <https://doi.org/10.1016/j.ensm.2020.01.011>.
105. Makiabadi, M.; Shamspur, T.; Mostafavi, A. Performance improvement of oxygen on the carbon substrate surface for dispersion of cobalt nanoparticles and its effect on hydrogen generation rate via NaBH₄ hydrolysis. *Int. J. Hydrogen Energy* **2020**, *45*, 1706–1718. <https://doi.org/10.1016/j.ijhydene.2019.11.026>.
106. Xu, Y.; Shan, W.; Liang, X.; Gao, X.; Li, W.; Li, H.; Qiu, X. Cobalt Nanoparticles Encapsulated in Nitrogen-Doped Carbon Shells: Efficient and Stable Catalyst for Nitrobenzene Reduction. *Ind. Eng. Chem. Res.* **2020**, *59*, 4367–4376. <https://doi.org/10.1021/acs.iecr.9b06604>.
107. Shu, H.; Lu, L.; Zhu, S.; Liu, M.; Zhu, Y.; Ni, J.; Ruan, Z.; Liu, Y. Ultra small cobalt nanoparticles supported on MCM41: One-pot synthesis and catalytic hydrogen production from alkaline borohydride. *Catal. Commun.* **2019**, *118*, 30–34. <https://doi.org/10.1016/j.cattcom.2018.09.012>.
108. Li, Y.; Hou, X.; Wang, J.; Feng, X.; Cheng, L.; Zhang, H.; Han, S. Co-Mo nanoparticles loaded on three-dimensional graphene oxide as efficient catalysts for hydrogen generation from catalytic hydrolysis of sodium borohydride. *Int. J. Hydrogen Energy* **2019**, *44*, 29075–29082. <https://doi.org/10.1016/j.ijhydene.2019.02.124>.
109. Rakap, M. Catalytic hydrolysis of hydrazine borane to release hydrogen by cobalt-ruthenium nanoclusters. *Int. J. Hydrogen Energy* **2020**, *45*, 15611–15617. <https://doi.org/10.1016/j.ijhydene.2020.04.042>.
110. Wang, Y.; Zou, K.; Zhang, D.; Cao, Z.; Zhang, K.; Xie, Y.; Zhou, G.; Li, G.; Bai, S. Cobalt–copper–boron nanoparticles as catalysts for the efficient hydrolysis of alkaline sodium borohydride solution. *Int. J. Hydrogen Energy* **2020**, *45*, 9845–9853. <https://doi.org/10.1016/j.ijhydene.2020.01.157>.
111. Wu, D.; Ye, P.; Wang, M.; Wei, Y.; Li, X.; Xu, A. Cobalt nanoparticles encapsulated in nitrogen-rich carbon nanotubes as efficient catalysts for organic pollutants degradation via sulfite activation. *J. Hazard. Mater.* **2018**, *352*, 148–156. <https://doi.org/10.1016/j.jhazmat.2018.03.040>.
112. Rasheed, T.; Nabeel, F.; Bilal, M.; Iqbal, H.M. Biogenic synthesis and characterization of cobalt oxide nanoparticles for catalytic reduction of direct yellow-142 and methyl orange dyes. *Biocatal. Agric. Biotechnol.* **2019**, *19*, 101154. <https://doi.org/10.1016/j.bcab.2019.101154>.
113. Zeng, Q.-X.; Xu, G.-C.; Zhang, L.; Lv, Y. Porous Cu₂O microcubes derived from a metal-formate framework as photocatalyst for degradation of methyl orange. *Mater. Res. Bull.* **2019**, *119*, 110537. <https://doi.org/10.1016/j.materresbull.2019.110537>.
114. Mapukata, S.; Kobayashi, N.; Kimura, M.; Nyokong, T. Asymmetrical and symmetrical zinc phthalocyanine-cobalt ferrite conjugates embedded in electrospun fibers for dual photocatalytic degradation of azo dyes: Methyl Orange and Orange G. *J. Photochem. Photobiol. A Chem.* **2019**, *379*, 112–122. <https://doi.org/10.1016/j.jphotochem.2019.04.048>.
115. Kaur, J.; Singhal, S. Facile synthesis of ZnO and transition metal doped ZnO nanoparticles for the photocatalytic degradation of Methyl Orange. *Ceram. Int.* **2014**, *40*, 7417–7424. <https://doi.org/10.1016/j.ceramint.2013.12.088>.
116. Dey, P.C.; Das, R. Enhanced photocatalytic degradation of methyl orange dye on interaction with synthesized ligand free CdS nanocrystals under visible light illumination. *Spectrochim. Acta Part A Mol. Biomol. Spectrosc.* **2020**, *231*, 118122. <https://doi.org/10.1016/j.saa.2020.118122>.
117. Naraginti, S.; Stephen, F.B.; Radhakrishnan, A.; Sivakumar, A. Zirconium and silver co-doped TiO₂ nanoparticles as visible light catalyst for reduction of 4-nitrophenol, degradation of methyl orange and methylene blue. *Spectrochim. Acta Part A Mol. Biomol. Spectrosc.* **2015**, *135*, 814–819. <https://doi.org/10.1016/j.saa.2014.07.070>.
118. Ahmad, I. Inexpensive and quick photocatalytic activity of rare earth (Er, Yb) co-doped ZnO nanoparticles for degradation of methyl orange dye. *Sep. Purif. Technol.* **2019**, *227*, 115726. <https://doi.org/10.1016/j.seppur.2019.115726>.
119. Dhas, C.R.; Venkatesh, R.; Jothivenkatachalam, K.; Nithya, A.; Benjamin, B.S.; Raj, A.M.E.; Jeyadheepan, K.; Sanjeeviraja, C. Visible light driven photocatalytic degradation of Rhodamine B and Direct Red using cobalt oxide nanoparticles. *Ceram. Int.* **2015**, *41*, 9301–9313. <https://doi.org/10.1016/j.ceramint.2015.03.238>.
120. El-Sayed, M.M.; Elsayed, R.E.; Attia, A.; Farghal, H.H.; Azzam, R.A.; Madkour, T.M. Novel nanoporous membranes of bio-based cellulose acetate, poly(lactic acid) and biodegradable polyurethane in-situ impregnated with catalytic cobalt nanoparticles for the removal of Methylene Blue and Congo Red dyes from wastewater. *Carbohydr. Polym. Technol. Appl.* **2021**, *2*, 100123. <https://doi.org/10.1016/j.carpta.2021.100123>.
121. Qi, Z.; Chen, L.; Zhang, S.; Su, J.; Somorjai, G.A. A mini review of cobalt-based nanocatalyst in Fischer-Tropsch synthesis. *Appl. Catal. A Gen.* **2020**, *602*, 117701. <https://doi.org/10.1016/j.apcata.2020.117701>.
122. Ralston, W.T.; Melaet, G.; Saephan, T.; Somorjai, G.A. Evidence of Structure Sensitivity in the Fischer-Tropsch Reaction on Model Cobalt Nanoparticles by Time-Resolved Chemical Transient Kinetics. *Angew. Chem. Int. Ed.* **2017**, *56*, 7415–7419. <https://doi.org/10.1002/anie.201701186>.

123. Luo, Q.-X.; Guo, L.-P.; Yao, S.-Y.; Bao, J.; Liu, Z.-T.; Liu, Z.-W. Cobalt nanoparticles confined in carbon matrix for probing the size dependence in Fischer-Tropsch synthesis. *J. Catal.* **2019**, *369*, 143–156. <https://doi.org/10.1016/j.jcat.2018.11.002>.
124. Bilal, M.; Mehmood, S.; Rasheed, T.; Iqbal, H.M.N. Bio-Catalysis and Biomedical Perspectives of Magnetic Nanoparticles as Versatile Carriers. *Magnetochemistry* **2019**, *5*, 42. <https://doi.org/10.3390/magnetochemistry5030042>.
125. Abbasi, B.A.; Iqbal, J.; Khan, Z.; Ahmad, R.; Uddin, S.; Shahbaz, A.; Zahra, S.A.; Shaukat, M.; Kiran, F.; Kanwal, S.; et al. Phytofabrication of cobalt oxide nanoparticles from *Rhamnus virgata* leaves extract and investigation of different bioactivities. *Microsc. Res. Tech.* **2021**, *84*, 192–201. <https://doi.org/10.1002/jemt.23577>.
126. Raeesi, M.; Alijani, H.Q.; Peydayesh, M.; Khatami, M.; Baravati, F.B.; Borhani, F.; Šlouf, M.; Soltaninezhad, S. Magnetic cobalt oxide nanosheets: Green synthesis and in vitro cytotoxicity. *Bioprocess Biosyst. Eng.* **2021**, *44*, 1423–1432. <https://doi.org/10.1007/s00449-021-02518-6>.
127. Verma, S.K.; Panda, P.K.; Kumari, P.; Patel, P.; Arunima, A.; Jha, E.; Husain, S.; Prakash, R.; Hergenröder, R.; Mishra, Y.K.; et al. Determining factors for the nano-biocompatibility of cobalt oxide nanoparticles: Proximal discrepancy in intrinsic atomic interactions at differential vicinage. *Green Chem.* **2021**, *23*, 3439–3458. <https://doi.org/10.1039/d1gc00571e>.
128. Kgosiemang, I.K.; Lefojane, R.; Direko, P.; Madlanga, Z.; Mashele, S.; Sekhoacha, M. Green synthesis of magnesium and cobalt oxide nanoparticles using *Euphorbia tirucalli*: Characterization and potential application for breast cancer inhibition. *Inorg. Nano-Metal Chem.* **2020**, *50*, 1070–1080. <https://doi.org/10.1080/24701556.2020.1735422>.
129. Farkas, B.; Santos-Carballal, D.; Cadi-Essadek, A.; de Leeuw, N.H. A DFT+U study of the oxidation of cobalt nanoparticles: Implications for biomedical applications. *Materialia* **2019**, *7*, 100381. <https://doi.org/10.1016/j.mtla.2019.100381>.
130. Maghsoudi, S.; Mohammadi, A. Reduced graphene oxide nanosheets decorated with cobalt oxide nanoparticles: A nonenzymatic electrochemical approach for glucose detection. *Synth. Met.* **2020**, *269*, 116543. <https://doi.org/10.1016/j.synthmet.2020.116543>.
131. Ren, Q.; Yang, K.; Zou, R.; Wan, Z.; Shen, Z.; Wu, G.; Zhou, Z.; Ni, Q.; Fan, W.; Hu, J.; et al. Biodegradable hollow manganese/cobalt oxide nanoparticles for tumor theranostics. *Nanoscale* **2019**, *11*, 23021–23026. <https://doi.org/10.1039/c9nr07725a>.
132. Li, Z.; Hu, S.; Liu, J.; Hu, Y.; Chen, L.; Jiang, T.; Sun, L.; Sun, Y.; Besenbacher, F.; Chen, C.; et al. Cobalt Phosphide Nanoparticles Applied as a Theranostic Agent for Multimodal Imaging and Anticancer Photothermal Therapy. *Part. Part. Syst. Charact.* **2018**, *35*, 1800127. <https://doi.org/10.1002/ppsc.201800127>.
133. Li, Z.; Li, Z.; Chen, L.; Hu, Y.; Hu, S.; Miao, Z.; Sun, Y.; Besenbacher, F.; Yu, M. Polyethylene glycol-modified cobalt sulfide nanosheets for high-performance photothermal conversion and photoacoustic/magnetic resonance imaging. *Nano Res.* **2018**, *11*, 2436–2449. <https://doi.org/10.1007/s12274-017-1865-z>.
134. Dhawan, U.; Tseng, C.-L.; Wang, H.-Y.; Hsu, S.-Y.; Tsai, M.-T.; Chung, R.-J. Assessing Suitability of Co@Au Core/Shell Nanoparticle Geometry for Improved Theranostics in Colon Carcinoma. *Nanomaterials* **2021**, *11*, 2048. <https://doi.org/10.3390/nano11082048>.
135. Ravichandran, M.; Oza, G.; Velumani, S.; Ramirez, J.T.; Garcia-Sierra, F.; Andrade, N.B.; Vera, A.; Leija, L.; Garza-Navarro, M.A. Plasmonic/Magnetic Multifunctional nanoplatform for Cancer Theranostics. *Sci. Rep.* **2016**, *6*, 34874. <https://doi.org/10.1038/srep34874>.
136. Huang, X.; Cai, H.; Zhou, H.; Li, T.; Jin, H.; Evans, C.; Cai, J.; Pi, J. Cobalt oxide nanoparticle-synergized protein degradation and phototherapy for enhanced anticancer therapeutics. *Acta Biomater.* **2021**, *121*, 605–620. <https://doi.org/10.1016/j.actbio.2020.11.036>.
137. Tian, J.; Zhu, H.; Chen, J.; Zheng, X.T.; Duan, H.; Pu, K.; Chen, P. Cobalt Phosphide Double-Shelled Nanocages: Broadband Light-Harvesting Nanostructures for Efficient Photothermal Therapy and Self-Powered Photoelectrochemical Biosensing. *Small* **2017**, *13*, 1700798. <https://doi.org/10.1002/sml.201700798>.
138. Shokrollahi, H. Structure, synthetic methods, magnetic properties and biomedical applications of ferrofluids. *Mater. Sci. Eng. C* **2013**, *33*, 2476–2487. <https://doi.org/10.1016/j.msec.2013.03.028>.
139. Li, X.; Zeng, C.; Jiang, J.; Ai, L. Magnetic cobalt nanoparticles embedded in hierarchically porous nitrogen-doped carbon frameworks for highly efficient and well-recyclable catalysis. *J. Mater. Chem. A* **2016**, *4*, 7476–7482. <https://doi.org/10.1039/c6ta01054g>.
140. Yao, Y.; Xu, C.; Qin, J.; Wei, F.; Rao, M.; Wang, S. Synthesis of Magnetic Cobalt Nanoparticles Anchored on Graphene Nanosheets and Catalytic Decomposition of Orange II. *Ind. Eng. Chem. Res.* **2013**, *52*, 17341–17350. <https://doi.org/10.1021/ie401690h>.
141. Michalek, F.; Lagunas, A.; Jimeno, C.; Pericàs, M.A. Synthesis of functional cobalt nanoparticles for catalytic applications. Use in asymmetric transfer hydrogenation of ketones. *J. Mater. Chem.* **2008**, *18*, 4692–4697. <https://doi.org/10.1039/b808383e>.
142. Liu, T.; Pang, Y.; Zhu, M.; Kobayashi, S. Microporous Co@CoO nanoparticles with superior microwave absorption properties. *Nanoscale* **2014**, *6*, 2447–2454. <https://doi.org/10.1039/c3nr05238a>.
143. Mohammadi, S.Z.; Darijani, Z.; Karimi, M.A. Fast and efficient removal of phenol by magnetic activated carbon-cobalt nanoparticles. *J. Alloys Compd.* **2020**, *832*, 154942. <https://doi.org/10.1016/j.jallcom.2020.154942>.
144. Roushani, M.; Baghelani, Y.M.; Mavaei, M.; Abbasi, S.; Mohammadi, S.Z. Preparation of Modified Magnetic Cobalt Nanoparticles as a New Magnetic Sorbent for the Preconcentration and Determination of Trace Amounts of Lead Ions in Environmental Water and Soil (Air-Dust) Samples. *Commun. Soil Sci. Plant Anal.* **2018**, *49*, 645–657. <https://doi.org/10.1080/00103624.2017.1417419>.
145. Zeisberger, M.; Dutz, S.; Müller, R.; Hergt, R.; Matoussevitch, N.; Bönnemann, H. Metallic cobalt nanoparticles for heating applications. *J. Magn. Magn. Mater.* **2007**, *311*, 224–227. <https://doi.org/10.1016/j.jmmm.2006.11.178>.
146. Leysens, L.; Vinck, B.; Van Der Straeten, C.; Wuyts, F.; Maes, L. Cobalt toxicity in humans—A review of the potential sources and systemic health effects. *Toxicology* **2017**, *387*, 43–56. <https://doi.org/10.1016/j.tox.2017.05.015>.

147. Renfrew, A.K.; O'Neill, E.S.; Hambley, T.; New, E.J. Harnessing the properties of cobalt coordination complexes for biological application. *Coord. Chem. Rev.* **2018**, *375*, 221–233. <https://doi.org/10.1016/j.ccr.2017.11.027>.
148. Nouri, M.; Esfahanizadeh, N.; Shahpar, M.G.; Attar, F.; Sartipnia, N.; Akhtari, K.; Saboury, A.A.; Falahati, M. Cobalt oxide nanoparticles mediate tau denaturation and cytotoxicity against PC-12 cell line. *Int. J. Biol. Macromol.* **2018**, *118*, 1763–1772. <https://doi.org/10.1016/j.ijbiomac.2018.07.024>.